International Journal of
Molecular Sciences

MDPI

Article

Stress Reactivity, Susceptibility to Hypertension, and Differential Expression of Genes in Hypertensive Compared to Normotensive Patients

Dmitry Oshchepkov [1], Irina Chadaeva [1], Rimma Kozhemyakina [1], Karina Zolotareva [1], Bato Khandaev [1], Ekaterina Sharypova [1], Petr Ponomarenko [1], Anton Bogomolov [1], Natalya V. Klimova [1], Svetlana Shikhevich [1], Olga Redina [1], Nataliya G. Kolosova [1], Maria Nazarenko [2], Nikolay A. Kolchanov [1], Arcady Markel [1] and Mikhail Ponomarenko [1,*]

[1] Institute of Cytology and Genetics, Siberian Branch of Russian Academy of Sciences, 630090 Novosibirsk, Russia; diman@bionet.nsc.ru (D.O.); ichadaeva@bionet.nsc.ru (I.C.); korimma@bionet.nsc.ru (R.K.); ka125699ri@yandex.ru (K.Z.); b.khandaev@g.nsu.ru (B.K.); sharypova@bionet.nsc.ru (E.S.); pon.petr@gmail.com (P.P.); mantis_anton@bionet.nsc.ru (A.B.); klimova@bionet.nsc.ru (N.V.K.); shikhsvt@bionet.nsc.ru (S.S.); oredina@bionet.nsc.ru (O.R.); kolosova@bionet.nsc.ru (N.G.K.); kol@bionet.nsc.ru (N.A.K.); markel@bionet.nsc.ru (A.M.)

[2] Institute of Medical Genetics, Tomsk National Research Medical Center, 634009 Tomsk, Russia; maria-nazarenko@medgenetics.ru

* Correspondence: pon@bionet.nsc.ru; Tel.: +7-(383)-363-4963 (ext. 1311)

Abstract: Although half of hypertensive patients have hypertensive parents, known hypertension-related human loci identified by genome-wide analysis explain only 3% of hypertension heredity. Therefore, mainstream transcriptome profiling of hypertensive subjects addresses differentially expressed genes (DEGs) specific to gender, age, and comorbidities in accordance with predictive preventive personalized participatory medicine treating patients according to their symptoms, individual lifestyle, and genetic background. Within this mainstream paradigm, here, we determined whether, among the known hypertension-related DEGs that we could find, there is any genome-wide hypertension theranostic molecular marker applicable to everyone, everywhere, anytime. Therefore, we sequenced the hippocampal transcriptome of tame and aggressive rats, corresponding to low and high stress reactivity, an increase of which raises hypertensive risk; we identified stress-reactivity-related rat DEGs and compared them with their known homologous hypertension-related animal DEGs. This yielded significant correlations between stress reactivity-related and hypertension-related fold changes (log2 values) of these DEG homologs. We found principal components, PC1 and PC2, corresponding to a half-difference and half-sum of these log2 values. Using the DEGs of hypertensive versus normotensive patients (as the control), we verified the correlations and principal components. This analysis highlighted downregulation of β-protocadherins and hemoglobin as whole-genome hypertension theranostic molecular markers associated with a wide vascular inner diameter and low blood viscosity, respectively.

Keywords: human; hypertension; stress reactivity; molecular marker; *Rattus norvegicus*; RNA-Seq; qPCR; differentially expressed gene; meta-analysis; correlation; principal component; bootstrap

check for updates

Citation: Oshchepkov, D.; Chadaeva, I.; Kozhemyakina, R.; Zolotareva, K.; Khandaev, B.; Sharypova, E.; Ponomarenko, P.; Bogomolov, A.; Klimova, N.V.; Shikhevich, S.; et al. Stress Reactivity, Susceptibility to Hypertension, and Differential Expression of Genes in Hypertensive Compared to Normotensive Patients. *Int. J. Mol. Sci.* **2022**, *23*, 2835. https://doi.org/10.3390/ijms23052835

Academic Editors: Iveta Bernatova, Monika Bartekova and Silvia Liskova

Received: 30 December 2021
Accepted: 28 February 2022
Published: 4 March 2022

Publisher's Note: MDPI stays neutral with regard to jurisdictional claims in published maps and institutional affiliations.

Copyright: © 2022 by the authors. Licensee MDPI, Basel, Switzerland. This article is an open access article distributed under the terms and conditions of the Creative Commons Attribution (CC BY) license (https://creativecommons.org/licenses/by/4.0/).

1. Introduction

Hypertension is a fatal yet preventable risk factor of ischemic heart disease [1], the top cause of death worldwide [2]. Besides essential hypertension, there are many cases of hypertension that are not clinically classified as essential. In all these cases, there is an increase in intravascular pressure (only local sometimes) together with vascular shear stress, oxidative stress, inflammatory reactions, and remodeling of the vascular wall. These pathogenic mechanisms common to all hypertensive conditions share, at least in part, a molecular basis that we are trying to pinpoint here.

Although the hypertensive risk increases with age [3,4], the age of the first clinical manifestations of hypertension is now diminishing [5]. Preeclampsia (hypertension in pregnancy) is becoming a challenge to obstetricians [6]. Prenatal stress can epigenetically reprogram a newborn's development and can lead to clinical hypertension in adulthood [7]. Pulmonary hypertension may start to develop in newborns [8]. Hypertension co-occurs with cancer [9–13], cirrhosis [14], and prostatitis [15]. Hypertension worsens both injury [16] and transplantation [17] of a kidney. Epilepsy [18], psoriasis, and dermatitis [19] are associated with hypertension. Anti–SARS-CoV-2 antibody titers are lower in hypertensive than in normotensive patients [20]. The "mosaic theory" of hypertension [21] was recently enriched with hypertensive development via exosome-dependent inflammation and angiogenesis impairment, associated with endothelial dysfunction and vascular remodeling [22]. A clinical review [23] revealed that the hypertensive risk increases with an increase in patients' stress reactivity [24]. Parents of half of the hypertensive patients had hypertension, but all the known (>60) hypertension-related whole-genome human loci explained only 3% of this heritability of hypertension [25]. Maybe this is why mainstream transcriptome-profiling studies on hypertensive versus normotensive patients [26–39] and animals [7,40–57] are focused on the differentially expressed genes (DEGs) that are specific to gender, age, and the stage of hypertension development. This is needed in predictive preventive personalized participatory (4P) medicine [58] to estimate where, how, why, and when hypertension might occur in a given patient depending on his/her genetic background. Because hypertension seems to have a finger in every pie, a meta-analysis of all the available specific hypertension-related DEGs can find among them a theranostic molecular marker of hypertension applicable to everyone, everywhere, anytime.

In our previous studies within this mainstream paradigm, we measured stress reactivity in rats [59] and created an inbred ISIAH rat strain (i.e., inherited stress-induced arterial hypertension) [60] and two outbred strains—tame and aggressive rats—corresponding to low and high stress reactivity [61–64]. On this basis, we sequenced transcriptomes in the brain stem [43], hypothalamus [44], renal medulla [45], renal cortex [46], and adrenal glands [47] of hypertensive ISIAH rats versus normotensive WAG rats. Besides this, we profiled transcriptomes of the hippocampus [40], prefrontal cortex [41], and retina [42] in OXYS rats (ICG SB RAS, Novosibirsk, Russia), which spontaneously develop the accelerated-senescence phenotype against a background of moderately high blood pressure [65–68] with respect to normotensive Wistar rats. In the present work, we meta-analyzed our eight abovementioned RNA-Seq datasets to ensure out of caution that among them (together with those available in PubMed [69]), there are still no invariant molecular markers of hypertension. Accordingly, we sequenced the hippocampal transcriptome of tame compared to aggressive rats and identified the stress-reactivity-related rat DEGs and—using our bioinformatics model [70–72]—compared them by homology with all the available hypertension-related animal DEGs that we could find. The results were verified using the DEGs of hypertensive versus normotensive patients.

2. Results

2.1. RNA-Seq and Mapping to the Reference Rat Genome

We sequenced the hippocampal transcriptome of three adult male tame gray rats (*Rattus norvegicus*)—in comparison with that of three aggressive ones—on an Illumina NextSeq 550 system (see Section 4.2). We chose the hippocampus because its functions contribute to learning under stress [73]. The rats were derived from two outbred tame and aggressive strains selectively bred at the ICG SB RAS [59,64] for over 90 generations using the glove test as described elsewhere [74]. The rats were not consanguineous (see Section 4.1). This procedure yielded 169,529,658 raw reads of 75 nt in length (Table 1); we deposited them in the NCBI SRA database [75] (ID PRJNA668014).

Table 1. Summary of searches for differentially expressed genes (DEGs) in hippocampal transcriptomes of three tame adult male rats (*Rattus norvegicus*) and three aggressive ones (all unrelated) in this work.

Group	Tame vs. Aggressive Rats
Total number of sequence reads (NCBI SRA ID: PRJNA668014)	169,529,658
Reads mapped to reference rat genome RGSC Rnor_6.0, UCSC Rn6, July 2014 (%)	146,521,467 (88.74%)
Expressed genes identified	14,039
Statistically significant DEGs ($P_{ADJ} < 0.05$, Fisher's Z-test with Benjamini correction)	42

In Table 1, the reader can see that 146,521,467 reads could be aligned with rat reference genome Rn6 and yielded 14,039 genes expressed within the hippocampus of the rats under study. Using Fisher's Z-test with Benjamini's correction for multiple comparisons, we found 42 DEGs that were not hypothetical, tentative, predicted, uncharacterized, or protein-non-coding genes; this approach reduced the false-positive error rates (Tables 1 and 2).

2.2. Quantitative PCR (qPCR)-Based Selective Verification of the DEGs Identified in this Work in the Hippocampus of Tame versus Aggressive Rats

First, we used 16 additional unrelated rats, namely: eight aggressive and eight tame rats that scored "–3" and "3", respectively, on a scale from –4 (most aggressive rat) to 4 (tamest rat) in the glove test [74] conducted one month before the extraction of hippocampus samples (Table 3). Next, among the 42 DEGs listed in Table 2, we chose *Ascl3* and *Defb17*; our qPCR data on them in the hippocampus of the tame and aggressive rats (see Section 4.4) are in Table 3 as the "mean ± standard error of the mean" ($M_0 \pm SEM$) of their expression relative to four reference genes (*B2m*, *Hprt1*, *Ppia*, and *Rpl30*) [76] in triplicate. Arithmetic-mean estimates of the expression levels of each gene (*Ascl3* and *Defb17)* in the hippocampus of these tame and aggressive rats in question are given in Table 3 and Figure 1a.

According to both the Mann–Whitney *U* test and Fisher's Z-test, both *Ascl3* and *Defb17* are significantly overexpressed in the hippocampus of the tame (white bars) versus aggressive (grey bars) rats according to the qPCR data obtained here (Figure 1a: $p < 0.05$, asterisks), consistently with the RNA-Seq data (Table 2). Figure 1b depicts a significant Pearson's linear correlation ($p < 0.00005$), Spearman's rank correlation ($p < 0.05$), and Kendall's rank correlation ($p < 0.05$) between the log2 values (hereinafter, log2: the log2-transformed ratio of an expression level of a given gene in tame rats to that in aggressive rats) for five genes—*Ascl3*, *Defb17*, *B2m*, *Ppia*, and *Rpl30* (open circles)—within the RNA-Seq (X-axis) and qPCR (Y-axis) data obtained here.

Table 2. The statistically significant DEGs in the hippocampus (of tame versus aggressive adult male rats) that were for the first time unidentified in this study.

#	Rat Gene, Name	*Symbol*	log2	*p*	P_{ADJ}
1	Albumin	*Alb*	3.21	$<10^{-11}$	$<10^{-7}$
2	Aquaporin 1 (Colton blood group)	*Aqp1*	5.91	$<10^{-6}$	$<10^{-2}$
3	Achaete-scute family bHLH transcription factor 3	*Ascl3*	2.38	$<10^{-4}$	<0.05
4	BAG cochaperone 3 (synonym: BCL2-associated athanogene 3)	*Bag3*	−0.92	$<10^{-4}$	<0.05
5	BAR/IMD domain-containing adaptor protein 2-like 1	*Baiap2l1*	3.67	$<10^{-4}$	<0.05
6	3-hydroxybutyrate dehydrogenase 1	*Bdh1*	0.40	$<10^{-4}$	<0.05
7	Cholecystokinin B receptor	*Cckbr*	1.24	$<10^{-8}$	$<10^{-4}$
8	Chondroitin sulfate proteoglycan 4B	*Cspg4b*	3.47	$<10^{-4}$	<0.05
9	Defensin β17	*Defb17*	5.94	$<10^{-4}$	<0.05
10	Ectonucleotide pyrophosphatase/phosphodiesterase 2	*Enpp2*	2.41	$<10^{-3}$	<0.05
11	Fras1-related extracellular matrix 1	*Frem1*	3.16	$<10^{-3}$	<0.05
12	Glycerol-3-phosphate dehydrogenase 1	*Gpd1*	−1.34	$<10^{-6}$	$<10^{-3}$
13	Hemoglobin, β adult major chain	*Hbb-b1*	−6.19	$<10^{-7}$	$<10^{-4}$
14	Hepatocyte nuclear factor 4α	*Hnf4a*	6.51	$<10^{-3}$	<0.05
15	5-hydroxytryptamine receptor 2C (synonym: serotonin receptor 2C)	*Htr2c*	2.03	$<10^{-3}$	<0.05
16	Keratin 2	*Krt2*	−1.43	$<10^{-6}$	$<10^{-3}$
17	Leukocyte immunoglobulin-like receptor, subfamily B, member 3-like	*Lilrb3l*	7.45	$<10^{-4}$	<0.05
18	Lymphocyte antigen 6 complex/Plaur domain-containing 1	*Lypd1*	−0.89	$<10^{-4}$	<0.05
19	MORN repeat-containing 1	*Morn1*	1.42	$<10^{-11}$	$<10^{-7}$
20	Myomesin 2	*Myom2*	−1.24	$<10^{-4}$	<0.05
21	Protocadherin β9	*Pcdhb9*	−1.03	$<10^{-4}$	<0.05
22	Protocadherin γ subfamily A1	*Pcdhga1*	2.45	$<10^{-4}$	<0.05
23	Prodynorphin	*Pdyn*	−0.89	$<10^{-4}$	<0.05
24	Phospholipase A2, group IID	*Pla2g2d*	2.84	$<10^{-4}$	<0.05
25	Phospholipase A2, group V	*Pla2g5*	3.85	$<10^{-4}$	<0.05
26	Procollagen-lysine, 2-oxoglutarate 5-dioxygenase 1	*Plod1*	−0.67	$<10^{-3}$	<0.05
27	Protein phosphatase 1, regulatory subunit 3B	*Ppp1r3b*	2.45	$<10^{-4}$	<0.05
28	Prolactin receptor	*Prlr*	6.43	$<10^{-5}$	$<10^{-2}$
29	Glycogen phosphorylase L	*Pygl*	−1.21	$<10^{-5}$	<0.05
30	RNA-binding motif protein 3	*Rbm3*	0.89	$<10^{-4}$	<0.05
31	Retinol saturase	*Retsat*	−0.98	$<10^{-4}$	<0.05
32	Solute carrier family 16, member 12	*Slc16a12*	3.08	$<10^{-3}$	<0.05
33	Solute carrier family 4, member 5	*Slc4a5*	6.27	$<10^{-6}$	$<10^{-3}$
34	SPARC-related modular calcium-binding 2	*Smoc2*	−2.09	$<10^{-4}$	<0.05
35	Serine peptidase inhibitor, Kunitz type 1	*Spint1*	−1.39	$<10^{-7}$	$<10^{-4}$
36	Sulfatase 1	*Sulf1*	3.72	$<10^{-6}$	$<10^{-2}$
37	Syncoilin, intermediate filament protein	*Sync*	1.17	$<10^{-3}$	<0.05
38	Tandem C2 domains, nuclear	*Tc2n*	3.47	$<10^{-5}$	$<10^{-2}$
39	Tectorin α	*Tecta*	1.38	$<10^{-8}$	$<10^{-5}$
40	Transmembrane protein 60	*Tmem60*	0.79	$<10^{-4}$	<0.05
41	Thioredoxin reductase 2	*Txnrd2*	−0.71	$<10^{-5}$	$<10^{-2}$
42	Uncoupling protein 2	*Ucp2*	0.73	$<10^{-4}$	<0.05

Note. Hereinafter, log2: the log2-transformed fold change (i.e., ratio of an expression level of a given gene in tame rats to that in aggressive rats); *p* and P_{ADJ}: statistical significance according to Fisher's Z-test without and with the Benjamini correction for multiple comparisons, respectively.

Table 3. qPCR data on the selected DEGs from the hippocampus of the independently obtained eight tame adult male rats and eight other aggressive ones (all unrelated animals).

Design		Behavioral "Glove" Test [74] and the qPCR Data on Gene Expression [This Work]								
Rat	**Set**	**No. 1**	**2**	**3**	**4**	**5**	**6**	**7**	**8**	
Glovetest	**A**	−3	−3	−3	−3	−3	−3	−3	−3	
	T	3	3	3	3	3	3	3	3	
DEG	**Set**	**Relative expression with respect to four reference genes, qPCR, $M_0 \pm$ SEM**								**TOTAL**
Ascl3	**A**	0.16 ± 0.02	0.88 ± 0.30	0.82 ± 0.08	0.09 ± 0.04	0.18 ± 0.03	0.07 ± 0.07	0.27 ± 0.11	0.32 ± 0.05	0.35 ± 0.17
	T	4.85 ± 4.38	3.40 ± 1.69	1.75 ± 0.24	2.21 ± 0.12	2.92 ± 0.05	4.48 ± 0.17	3.83 ± 0.33	2.64 ± 0.15	3.26 ± 1.71
Defb17	**A**	0.005 ± 0.005	0.01 ± 0.005	0.005 ± 0.005	0.005 ± 0.005	0.005 ± 0.005	ND	0.005 ± 0.005	0.005 ± 0.005	0.01 ± 0.01
	T	1.72 ± 0.04	3.22 ± 0.42	2.52 ± 0.14	1.82 ± 0.55	2.45 ± 0.10	4.43 ± 0.26	1.99 ± 0.89	2.34 ± 0.27	2.56 ± 0.53

Note. Sets: A, aggressive rats; T, tame rats; qPCR data: "$M_0 \pm$ SEM" denotes the mean ± standard error of the mean for three technical replicates for each rat; ND, not detected.

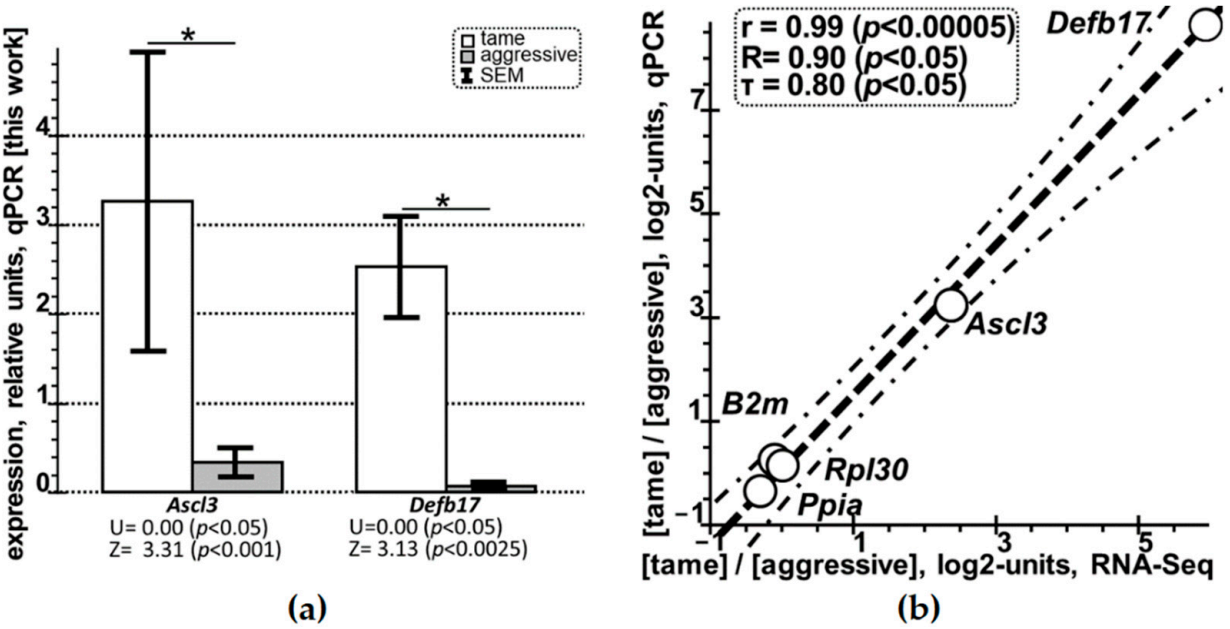

Figure 1. qPCR-based selective verification of the DEGs identified by RNA-Seq in this work in the hippocampus of tame versus aggressive rats. *Legend*: (**a**) in tame male adult rats (white bars) versus aggressive ones (grey bars), both DEGs examined (i.e., *Ascl3* and *Defb17*) are statistically significantly overexpressed in the hippocampus (here, bar height (i.e., mean), error bars (i.e., standard error of the mean [SEM]), and asterisks denote statistical significance at $p < 0.05$ according to both the nonparametric Mann–Whitney *U*-test and parametric Fisher's *Z*-test). Asterisk (symbol "*"), statistically significant at $p < 0.05$. (**b**) Statistically significant correlations between the relative expression levels of the two selected DEGs and three reference genes (i.e., *B2m* (β-2-microglobulin), *Ppia* (peptidylprolyl isomerase A), and *Rpl30* (ribosomal protein L30)) in the hippocampus of tame versus aggressive rats (open circles), as measured experimentally by RNA-Seq (X-axis) and qPCR (Y-axis) and presented on the log2 scale (see "Materials and Methods"). Dashed and dash-and-dot lines denote linear regression and boundaries of its 95% confidence interval calculated using Statistica software (Statsoft^{TM}, Tulsa, OK, USA). r, R, τ, and *p* are coefficients of Pearson's linear correlation, Spearman's rank correlation, Kendall's rank correlation, and their *p* values (statistical significance), respectively.

2.3. Comparison of the Known DEGs (of Hypertensive versus Normotensive Animals) with Their Homologous Genes among the 42 Hippocampal DEGs (of Tame versus Aggressive Rats) Identified Here

In this study, using the PubMed database [69], we compiled all the transcriptomes (that we could find) of hypertensive versus normotensive animals, as presented in Table 4. The total number of DEGs was 4216 in 14 tissues of four animal species, as cited in the rightmost column of Table 4 [7,40–57].

Table 4. The DEGs—of hypertensive versus normotensive animals—that we could find (available in PubMed [69]).

#	Species	Hypertensive	Normotensive	Tissue	N_{DEG}	Ref.
1	rat	OXYS	Wistar	hippocampus	85	[40]
2	rat	OXYS	Wistar	prefrontal cortex	73	[41]
3	rat	OXYS	Wistar	retina	85	[42]
4	rat	ISIAH	WAG	brain stem	206	[43]
5	rat	ISIAH	WAG	hypothalamus	137	[44]
6	rat	ISIAH	WAG	renal medulla	882	[45]
7	rat	ISIAH	WAG	renal cortex	309	[46]
8	rat	ISIAH	WAG	adrenal gland	1020	[47]
9	rat	SHR	Wistar	brain pericytes	21	[48]
10	rat	SHR	Wistar	kidney	35	[49]
11	rat	SD, monocrotaline-treated	SD, saline-treated	lung	10	[50]
12	rat	Dahl-SS, water after salt diet	Dahl-SS, QSYQ after salt diet	kidney	13	[51]
13	rat	*Resp18*-null Dahl-SS	Dahl-SS	kidney	14	[52]
14	rat	prenatal dexamethasone stress	norm	adrenal gland	93	[7]
15	mice	*Toxoplasma* infection in pregnancy	norm	uterus	10	[53]
16	mice	BPH/2J	BPN/3J	kidney	883	[54]
17	rabbit	G2K1C-treated	norm	middle cerebral artery	230	[55]
18	chicken	high (1.2%) Ca diet	normal (0.8%) Ca diet	kidney	92	[56]
19	chicken	cold stress with salt diet	healthy chicken	pulmonary arteries	18	[57]
Σ	4 species	14 animal models of human hypertension		14 tissues	4216	

Note. N_{DEG}: the number of DEGs; BPH/2J, BPN/3J Dahl-SS, ISIAH, OXIS, SD, SHR, WAG, and Wistar: laboratory animal strains; QSYQ: QiShenYiQi pills, a cardioprotective remedy from traditional Chinese medicine; G2K1C: Goldblatt 2-kidney 1-clip; Ref.: reference.

Figure S1 (hereinafter: see Supplementary Materials) depicts how we compared 4216 DEGs of hypertensive versus normotensive animals (Table 4) with 42 hippocampal DEGs of the tame versus aggressive rats (Table 2). First, we compiled 151 pairs of homologous DEGs, where one DEG was taken from Table 2, while its homologous DEG was found among the 4216 DEGs described in Table 4 (both are in Table S1 (hereinafter: see Supplementary Materials)), as shown in Figure S1 using a Venn diagram and in the table. Next, for the first time. we found that stress-reactivity-related and hypertension-related log2 values of the homologous animal DEGs statistically significantly correlate with each other according to Pearson's linear correlation ($r = -0.29$, $p < 0.0005$), the Goodman–Kruskal generalized correlation ($\gamma = -0.20$, $p < 0.0005$), and Spearman's ($R = -0.29$, $p < 0.00025$) and Kendall's ($\tau = -0.20$, $p < 0.0005$) rank correlations. Finally, we processed Table S1 by principal component analysis in the Bootstrap mode of the PAST4.04 software [77] that yielded principal components PC1 and PC2, corresponding to a half-difference and half-sum of the stress reactivity-related and hypertension-related log2 values of the homologous animal DEGs (Figure S1).

2.4. Verification of the Results Obtained on the Hypertensive versus Normotensive Animals Examined in this Work with respect to the DEGs—Of Hypertensive versus Normotensive Patients—That We Could Find

Using the PubMed database [69], we collected all the DEGs (of hypertensive compared with normotensive patients) that we could find (Table 5). The total number of hypertension-related human DEGs found was 7865, as cited in the rightmost column of Table 5 [26–39].

Table 5. The analyzed DEGs—of hypertensive versus normotensive patients—that we could find (available in PubMed [69]).

#	Hypertensive	Normotensive	Tissue	N_{DEG}	Ref.
1	renal medullary hypertension	norm	renal medulla	13	[26]
2	pulmonary arterial hypertension	norm	lung	49	[27]
3	pulmonary arterial hypertension	norm	lung	119	[28]
4	men with pulmonary arterial hypertension	normal men	blood	14	[29]
5	women with pulmonary arterial hypertension	normal women	blood	15	[29]
6	pulmonary hypertension during pulmonary fibrosis	norm	lung	3520	[30]
7	*BMPR2*-deficient human cells	normal cells	pulmonary artery endothelial cells	483	[31]
8	preeclampsia	normal pregnant	placenta	1228	[32]
9	preeclampsia	normal pregnant	placenta	10	[33]
10	preeclampsia	normal pregnant	venous blood	64	[34]
11	preeclampsia	normal pregnant	decidua basalis	372	[35]
12	excessive miR-210 in SWAN-71 cells	normal SWAN-71 cells	trophoblast cell line SWAN-71	19	[36]
13	hypertension-induced nephrosclerosis	norm	kidney	16	[37]
14	hypertension-related pre-invasive squamous cancer	normal cells, the same biopsies	squamous lung cancer cells	119	[38]
15	hypertension-induced atrial fibrillation	norm	auricle tissue biopsy	300	[39]
16	hypertension-induced coronary artery disease	norm	peripheral blood	1524	[39]
Σ	10 human hypertension-related disorders		12 tissues	7865	

Note. See the footnote of Table 4.

Figure 2 shows exactly how we reproduced step-by-step the results obtained from the hypertension-related animal DEGs only by replacing them with the hypertension-related human DEGs (Table 5) as independent control clinical data that are documented in Table S2. The lower half of this figure presents robust correlations between the stress-reactivity-related and hypertension-related log2 values corresponding to animal and human DEG homologs as well as principal components PC1 and PC2 proportional to the half-difference and half-sum, respectively, of these log2 values; this was the essence of the verification.

2.5. Searching for the Hypertension-Related Molecular Markers among the Human Genes Orthologous to the 42 Hippocampal DEGs (of Tame versus Aggressive Rats) Identified in this Work

To this end, first of all, using the PubMed database [69], we characterized each of the 42 hippocampal DEGs (of tame versus aggressive rats) identified in this work (Table 2), in terms of how downregulation or upregulation of their orthologous human genes can manifest itself in hypertension, as presented [78–186] in Table S3 (hereinafter: see Supplementary Materials).

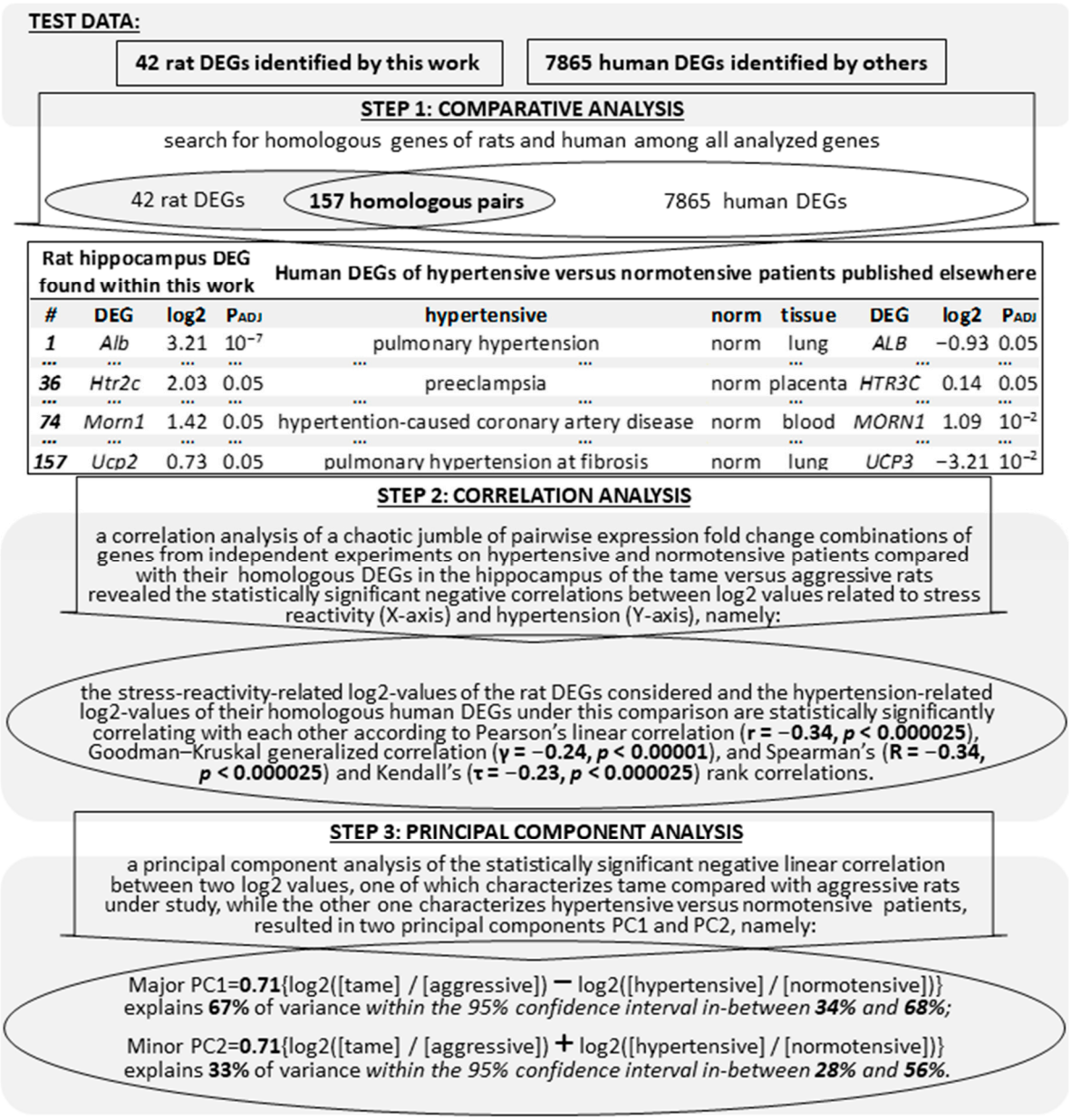

Figure 2. A step-by-step diagram of verification of the obtained results on the hypertensive versus normotensive animals examined in this work with respect to all the transcriptomes (that we could find) of hypertensive versus normotensive patients (Table 5). *Legend*: see the footnote of Table 2; PC1 and PC2: principal components calculated using the PAST4.04 software [77].

Next, for each hippocampal DEG (of tame versus aggressive rats) in question (Table 2), we determined how many homologous DEGs of hypertensive versus normotensive subjects (i.e., patients and animals) have the opposite (N_{PC1}) or the same (N_{PC2}) sign of their log2 values related to hypertension, as compared with the sign of the log2 value of this hippocampal DEG in tame versus aggressive rats, because principal components PC1 and PC2 correspond to a half-difference and half-sum, respectively, of these log2 values (Figure S1 and Figure 2).

Table 6 presents these determined quantities (N_{PC1} and N_{PC2}) together with their statistical significance assessed via the binomial distribution both without (*p*-values) and with (P_{ADJ}-values) Bonferroni's correction for multiple comparisons.

Table 6. Searching for hypertension-related molecular markers among the human genes orthologous to the 42 hippocampal DEGs (of tame versus aggressive rats) identified in this work. Here, we took into account the number of their homologous DEGs in the tissues of hypertensive versus normotensive subjects (patients and animals).

Rat Gene		Total Number of DEGs		Binomial Distribution		Rat Gene		Total Number of DEGs		Binomial Distribution	
#	*Symbol*	N_{PC1}: Opposite Signs	N_{PC2}: Matching Signs	*p*	P_{ADJ}	#	*Symbol*	N_{PC1}: Opposite Signs	N_{PC2}: Matching Signs	*p*	P_{ADJ}
i	ii	iii	iv	v	vi	i	ii	iii	iv	v	vi
1	*Alb*	1	1	0.75	1.00	*22*	*Pcdhga1*	1	1	0.75	1.00
2	*Aqp1*	6	6	0.61	1.00	*23*	*Pdyn*	0	0	ND	ND
3	*Ascl3*	1	1	0.75	1.00	*24*	*Pla2g2d*	19	12	0.14	1.00
4	*Bag3*	2	2	0.69	1.00	*25*	*Pla2g5*	19	12	0.14	1.00
5	*Baiap2l1*	1	0	0.50	1.00	*26*	*Plod1*	3	1	0.31	1.00
6	*Bdh1*	2	0	0.25	1.00	*27*	*Ppp1r3b*	2	3	0.50	1.00
7	*Cckbr*	1	0	0.50	1.00	*28*	*Prlr*	0	1	0.50	1.00
8	*Cspg4b*	0	0	ND	ND	*29*	*Pygl*	0	1	0.50	1.00
9	*Defb17*	2	3	0.50	1.00	*30*	*Rbm3*	15	12	0.35	1.00
10	*Enpp2*	3	8	0.11	1.00	*31*	*Retsat*	5	2	0.23	1.00
11	*Frem1*	1	1	0.75	1.00	*32*	*Slc16a12*	7	6	0.50	1.00
12	*Gpd1*	4	1	0.19	1.00	*33*	*Slc4a5*	7	5	0.83	1.00
13	*Hbb-b1*	24	3	10^{-4}	10^{-3}	*34*	*Smoc2*	3	1	0.31	1.00
14	*Hnf4a*	0	0	ND	ND	*35*	*Spint1*	1	1	0.75	1.00
15	*Htr2c*	3	3	0.65	1.00	*36*	*Sulf1*	0	0	ND	ND
16	*Krt2*	22	13	0.09	1.00	*37*	*Sync*	0	0	ND	ND
17	*Lilrb3l*	10	1	10^{-2}	0.24	*38*	*Tc2n*	2	0	0.25	1.00
18	*Lypd1*	11	7	0.24	1.00	*39*	*Tecta*	0	1	0.50	1.00
19	*Morn1*	0	4	0.06	1.00	*40*	*Tmem60*	0	0	ND	ND
20	*Myom2*	2	1	0.50	1.00	*41*	*Txnrd2*	2	0	0.25	1.00
21	*Pcdhb9*	10	0	10^{-3}	0.05	*42*	*Ucp2*	1	1	0.75	1.00

Note. *p* and P_{ADJ}: a significance estimate according to the binomial distribution without or with Bonferroni's correction for multiple comparisons, respectively; ND: not detected; underlining: statistically significant hypertension-related molecular markers identified in this work.

As shown in this table, only two of the 42 DEGs (in the hippocampus of the tame versus aggressive rats) found here are linked with PC1 (i.e., *Hbb-b1* and *Pcdhb9*, as described in Table 7). Looking through Table 7, readers can see the statistically significant upregulation of both β-protocadherin and hemoglobin subunit DEGs in the tissues of the hypertensive versus normotensive subjects (patients and animals). This result allowed us to propose the statistically significant downregulation of their homologous DEGs (in the hippocampus of tame versus aggressive rats), identified here (Table 2) as candidate hypertension theranostic molecular markers.

2.6. Verification of Downregulation of Human β-Hemoglobin and β-Protocadherins as HypertensionTtheranostic Molecular Markers using the DEGs (That We Could Find) of Domestic versus Wild Animals

For this purpose, using the PubMed database [69], we collected all the transcriptomes (that we could find) of domestic animals compared with their wild congeners, as shown in Table 8. The bottom row of this table indicates that we found 2393 DEGs in the tissues of domestic versus wild animals, as cited in the rightmost column of this table [72,187–193].

Table 7. Statistically significant upregulation of the hemoglobin subunit and β-protocadherin DEGs—in the tissues of the hypertensive versus normotensive subjects (i.e., patients and animals)—that were for the first time compiled together here.

#	Species	Hypertensive	Normotensive	Tissue	*DEG*	log2	P_{ADJ}	Ref.
i	ii	iii	iv	v	v	vi	vii	viii
1	rat	ISIAH	WAG	brain stem	*Hbb-b1*	1.42	10^{-2}	[43]
2	rat	ISIAH	WAG	hypothalamus	*Hbb-b1*	2.02	10^{-2}	[44]
3	rat	ISIAH	WAG	renal medulla	*Hbb-b1*	1.18	10^{-2}	[45]
4	rat	ISIAH	WAG	adrenal gland	*Hbb-b1*	1.32	10^{-2}	[47]
5	rat	ISIAH	WAG	adrenal gland	*Hba2*	0.69	10^{-2}	[47]
6	rat	ISIAH	WAG	adrenal gland	*Hbb*	2.02	10^{-2}	[47]
7	rat	ISIAH	WAG	adrenal gland	*Hbb-m*	3.78	10^{-2}	[47]
8	rat	ISIAH	WAG	brain stem	*Hba2*	0.58	0.05	[43]
9	rat	ISIAH	WAG	brain stem	*Hbb*	1.88	10^{-2}	[43]
10	rat	ISIAH	WAG	brain stem	*Hbb-m*	3.65	10^{-2}	[43]
11	rat	ISIAH	WAG	hypothalamus	*Hba1*	1.14	10^{-2}	[44]
12	rat	ISIAH	WAG	hypothalamus	*Hba2*	1.32	10^{-2}	[44]
13	rat	ISIAH	WAG	hypothalamus	*Hbb*	3.23	10^{-2}	[44]
14	rat	ISIAH	WAG	hypothalamus	*Hbb-m*	1.09	10^{-2}	[44]
15	rat	ISIAH	WAG	renal medulla	*Hbb*	−0.68	10^{-2}	[45]
16	rat	ISIAH	WAG	renal medulla	*Hbb-m*	2.72	10^{-2}	[45]
17	rat	ISIAH	WAG	renal medulla	*Hbb-s*	2.38	10^{-2}	[45]
18	human	preeclampsia	norm	placenta	*HBD*	−0.63	10^{-3}	[32]
19	human	pulmonary hypertension during pulmonary fibrosis	norm	lungs	*HBD*	−2.83	10^{-3}	[30]
20	human	pulmonary hypertension	norm	lungs	*HBA1*	2.08	10^{-9}	[28]
21	human	pulmonary hypertension	norm	lungs	*HBB*	2.46	10^{-10}	[28]
22	human	HT-induced coronary disease	norm	peripheral blood	*HBBP1*	1.03	0.05	[39]
23	human	HT-induced coronary disease	norm	peripheral blood	*HBE1*	1.42	0.05	[39]
24	human	HT-induced coronary disease	norm	peripheral blood	*HBG2*	4.49	0.05	[39]
25	human	HT-induced coronary disease	norm	peripheral blood	*HBM*	5.33	0.05	[39]
26	human	HT-induced coronary disease	norm	peripheral blood	*HBQ1*	3.10	0.05	[39]
27	human	HT-induced atrial fibrillation	norm	auricle tissue biopsy	*HBA2*	2.37	10^{-2}	[39]
28	rat	ISIAH	WAG	brain stem	*Pcdhb7*	1.60	10^{-2}	[43]
29	mouse	BPH/2J	BPN/3J	kidneys	*Pcdhb16*	1.22	10^{-3}	[54]
30	human	pulmonary hypertension during pulmonary fibrosis	norm	lungs	*PCDHB10*	1.89	10^{-2}	[30]
31	human	pulmonary hypertension during pulmonary fibrosis	norm	lungs	*PCDHB15*	1.47	10^{-4}	[30]
32	human	pulmonary hypertension during pulmonary fibrosis	norm	lungs	*PCDHB16*	1.38	10^{-4}	[30]
33	human	pulmonary hypertension during pulmonary fibrosis	norm	lungs	*PCDHB17P*	1.21	10^{-2}	[30]
34	human	pulmonary hypertension during pulmonary fibrosis	norm	lungs	*PCDHB4*	2.93	10^{-4}	[30]
35	human	pulmonary hypertension during pulmonary fibrosis	norm	lungs	*PCDHB6*	1.35	10^{-2}	[30]
36	human	HT-induced coronary disease	norm	peripheral blood	*PCDHB11*	1.12	0.05	[39]
37	human	HT-induced coronary disease	norm	peripheral blood	*PCDHB13*	1.04	0.05	[39]

Notes. HT, hypertension.

Table 8. The investigated genome-wide RNA-Seq transcriptomes (of domestic animals with their wild congeners) that we could find in the PubMed database [69].

#	Domestic Animals	Wild Animals	Tissue	N_{DEG}	Ref.
1	tame rats	aggressive rats	hypothalamus	46	[72]
2	tame rats	aggressive rats	frontal cortex	20	[187]
3	guinea pigs	cavy	frontal cortex	883	[187]
4	domestic rabbits	wild rabbits	frontal cortex	17	[187]
5	domestic rabbits	wild rabbits	parietal-temporal cortex	216	[188]
6	domestic rabbits	wild rabbits	amygdala	118	[188]
7	domestic rabbits	wild rabbits	hypothalamus	43	[188]
8	domestic rabbits	wild rabbits	hippocampus	100	[188]
9	dogs	wolves	blood	450	[189]
10	dogs	wolves	frontal cortex	13	[187]
11	tame foxes	aggressive foxes	pituitary	327	[190]
12	pigs	boars	frontal cortex	30	[187]
13	pigs	boars	frontal cortex	34	[191]
14	pigs	boars	pituitary	22	[192]
15	domestic chicken	wild chicken	pituitary	474	[193]
Σ	7 domestic animal species	7 wild animal species	8 tissues	2393	

Using the 42 DEGs (from the hippocampus of the tame versus aggressive rats) identified here (Table 2), together with these 2393 DEGs of domestic versus wild animals (Table 8), we revealed three β-protocadherin DEGs and seven hemoglobin subunit DEGs, which are compared in Table 9 with the human homologous genes (*HBB*, *HBD*, and *PCDHB9*), annotated with respect to hypertension in Table S3. Within columns viii and ix of this table, we transformed the log2 value characterizing the animal hemoglobin subunit and β-protocadherin DEGs into either underexpression or overexpression of the corresponding gene during divergence of domestic and wild animals from their most recent common ancestor, which is the most widely used phylogeny concept [194–198]. Downregulation of human genes *HBB* and *HBD* reduces blood viscosity [199] and corresponds to downregulation of the homologous genes *Hbb-b1*, *Hbbl*, *Hba1*, *Hbad*, *Hbm*, and *Hbz1* in the tame rat, domestic chicken, or dog during their divergence from their most recent ancestors with respect to their wild congeners (Table 9). As for human hemoglobin upregulation, a high-altitude environment provokes both hypertension and hyperhemoglobinemia [103]. This hemoglobin upregulation in humans corresponds to high hemoglobin subunit levels in aggressive rats [72], wolves [189], and wild chickens [193] during their microevolution (Table 9). Likewise, human gene *PCDHB9* (protocadherin β9) downregulation leads to a wide vascular inner diameter [200] and corresponds to downregulation of β-protocadherins in tame rats [72] and domestic rabbits [188] during their microevolution (Table 9). Finally, PCDHB9 upregulation in humans elevates the risk of gastric cancer [201] (the surgical removal of which leads to hypertensive remission [12]) and corresponds to upregulation of β-protocadherins in aggressive rats [72] and wild rabbits [188] during their microevolution (Table 9). As a standard Fisher's 2 × 2 table, Table 10 summarizes the observations detailed in Table 9.

As one can see in Table 10, downregulation of the genes of β-protocadherins and hemoglobin subunits, which were associated with a wide vascular inner diameter [200] and low blood viscosity [199], respectively, was observed only in domestic animals (not in their wild congeners). This difference is statistically significant according to the binomial distribution ($p < 0.0001$), Pearson's χ^2 test ($p < 0.001$), and Fisher's exact test ($p < 0.001$). Thus, downregulation of β-protocadherins and downregulation of hemoglobin subunits in animals are molecular markers of low stress reactivity [24], which is both a key physiological trait for domestic animals [61,62] and a clinically proven hypertension theranostic physiological marker in everyone, everywhere, anytime [23].

Table 9. Comparing the effects of changes to the expression of homologous genes (a) on hypertension development in humans and (b) during the divergence of domestic and wild animals from their most recent common ancestors.

	(a) Humans				**(b) Animals**					
Gene	**Effect of Gene Expression Changes on Hypertension (HT): Hypertensive (→) or Normotensive (←)**				**RNA-Seq**		**Effect of Gene Expression Changes during Divergence from the Most Recent Common Ancestor**			**Ref.**
	Downregulation	**HT**	**Upregulation**	**HT**	***DEG***	**log2**	**Downregulation**	**Upregulation**	**Tissue**	
i	**ii**	**iii**	**iv**	**v**	**vi**	**vii**	**viii**	**ix**	**x**	**xi**
HBB, HBD	low blood viscosity [199]	←	high-altitude environment provokes hyperhemoglobinemia and hypertension [103]	→	*Hbb-b1*	−6.19	tame rat	aggressive rat	hippocampus	[this work]
					Hbb-b1	−3.97	tame rat	aggressive rat	hypothalamus	[72]
					Hbbl	−5.92	dogs	wolves	blood	[189]
					Hba1	−4.06	dogs	wolves	blood	[189]
					Hbad	−1.07	domestic chickens	wild chickens	pituitary	[193]
					Hbm	−6.46	dogs	wolves	blood	[189]
					Hbz1	−7.10	dogs	wolves	blood	[189]
PCDHB9	wide vascular inner diameter [200]	←	higher risks of gastric cancer [93], surgical removal of which relieves hypertension [12]	→	*Pcdhb9*	−1.03	tame rat	aggressive rat	hippocampus	[this work]
					Pcdhb9	−1.01	tame rat	aggressive rat	hypothalamus	[72]
					Pcdhb15	−1.04	domestic rabbits	wild rabbits	parietal-temporal cortex	[188]

Table 10. Correlations between the effects of unidirectional changes in the expression of homologous genes (a) on human hypertension and (b) during the divergence of studied domestic and wild animals from their most recent common ancestor.

(b) Animals	(a) Humans	Effect of Expression Changes of Genes Encoding Hemoglobin Subunits and β-Protocadherins in Patients		Binomial Distribution	Pearson's χ^2 Test		Fisher's Exact Test
		Hypertensive	Normotensive		χ^2	p	
Effect of expression changes of genes encoding hemoglobin subunits and β-protocadherins during animal microevolution	wild	10	0	10^{-4}	20.00	10^{-3}	10^{-5}
	domestic	0	10	10^{-4}			

3. Discussion

Here, we observed for the first time that downregulation of hemoglobin subunits or β-protocadherins corresponds to low blood viscosity or a wide vascular inner diameter, i.e., two universal genome-wide hypertension theranostic molecular markers applicable to everyone, everywhere, anytime, as readers can see in Table 7. Because of atherosclerosis comorbid with hypertension, this may support our previous finding that natural selection against underexpression of atheroprotective genes slows atherogenesis [202].

Nevertheless, it seems to be highly debatable how low expression levels of human genes *HBB*, *HBD*, and *PCDHB9* would be adaptive under natural selection, favoring their downregulation that could cause their loss. For this reason, here, we analyzed these genes using our web service SNP_TATA_Comparator [203] applicable to research on hypertension, owing to its successful use in a clinical study on pulmonary tuberculosis [204] comorbid with hypertension [205]. Figure S2 exemplifies how we also used the UCSC Browser [206], Bioperl toolkit [207], and a package of R [208], together with both Ensembl [209] and dbSNP [210] databases in the case of the candidate SNP marker (rs34166473) reducing blood viscosity via *HBD* downregulation [199], as outlined here (Table S4). In total, we examined all 85 SNPs within the 70 bp proximal promoters of the genes *HBD*, *HBD*, and *PCDHB9* within build #153 of the dbSNP database [210]. As a result of this work, we found 27 candidate SNP markers of hypertension, as indicated [12,103,199–201,211] in Table S4 and described [212–220] in Section S1 "Supplementary methods for DNA sequence analysis" (see Supplementary Materials).

Besides this, Figure S3 (hereinafter: see Supplementary Materials) presents the selective experimental verification [221–223] of these estimates (in an electrophoretic mobility shift assay; EMSA) exemplified by minor allele −30C of rs1473693473 (see Section S2 "Supplementary methods for in vitro measurements"). In total, we verified two ancestral alleles of the human *HBB* and *HBD* genes along with nine minor alleles, namely: rs35518301:g, rs34166473:c, rs34500389:t, rs33980857:a, rs34598529:g, rs33931746:g, rs33931746:c, rs281864525:c, and rs63750953:deletion (Table S5 (hereinafter: see Supplementary Materials)). According to Goodman–Kruskal generalized correlation (γ), Pearson's linear correlation (r), and Spearman's (R) and Kendall's (τ) rank correlations, our computational predictions and experimental measurements are in significant agreement with one another (Figure S3c).

Finally, according to the semicentennial tradition, to assess the relative mutation rates (e.g., transitions versus transversions [224], synonymous versus non-synonymous substitutions [225], and insertions versus deletions [226]), we compared the genes *HBB*, *HBD*, and *PCDHB9* in question with the human genome as a whole [227–229] (Table 11).

Table 11. The hypertension-related candidate SNP markers within *HBB*, *HBD*, and *PCDHB9* promoters (predicted here) and their comparison with genome-wide patterns.

Data: GRCh38, dbSNP rel. 153 [210]				**H_0: Neutral Drift [229,230]**			**H_0: "→HT and ←HT Equivalence"**		
SNPs	N_{GENE}	N_{SNP}	N_{RES}	$N_{>}$	$N_{<}$	$p(H_0: N_{>} < N_{<})$ [227]	$N_{\rightarrow HT}$	$N_{\leftarrow HT}$	$p(H_0: N_{\rightarrow HT} \equiv N_{\leftarrow HT})$
Whole-genome norm for SNPs of TBP sites [228]	10^4	10^5	10^3	200	800	>0.99	-	-	-
HT-related candidate SNP markers at TBP sites [this work]	3	85	27	8	19	>0.99	8	19	<0.05

Notes. Hypertension (HT): normotensive (←HT) and hypertensive (→HT). N_{GENE} and N_{SNP}: total numbers of the human genes and of their SNPs meeting the criteria for this study. N_{RES}: the total number of the candidate SNP markers that can increase ($N_{>}$) or decrease ($N_{<}$) the affinity of TATA-binding protein (TBP) for these promoters and to respectively affect the expression of these genes. $N_{\leftarrow HT}$ and $N_{\rightarrow HT}$: total numbers of the candidate SNP markers that can prevent or provoke hypertension. $p(H_0)$: the estimate of probability for the acceptance of this H_0 hypothesis, in accordance with the binomial distribution. TBP-site: TATA-binding-protein binding site.

At the top of this table is a genome-wide SNP pattern of TBP sites—where SNPs decreasing the TBP–DNA affinity dominate over SNPs, thus increasing this affinity within the human genome—as predicted by taking into account many mutagenesis molecular mechanisms (e.g., epistatic effects) [227] and as proven within the "1000 Genomes" project [228]. In accordance with Haldane's dilemma [229] and neutral evolution theory [230], this whole-genome trait reflects neutral mutation drift as a norm. At the bottom of Table 11 is the hypertension-related candidate SNP markers identified here, which often significantly reduce the affinity of TBP for promoters of the genes *HBB*, *HBD*, and *PCDHB9*, representing the genome-wide neutral mutational drift antagonizing hypertension.

Altogether, the hypertension-related candidate SNP markers discussed above fit the newest concept [231]: in addition to the accumulation of degenerative SNPs owing to their uncontrollability during neutral mutational drift, some adaptive SNPs can also accumulate in this way (Table 11).

4. Materials and Methods

4.1. Animals

The study was conducted on adult male gray rats (*R. norvegicus*) artificially bred for over 90 generations for either aggressive or tame behavior (as two outbred strains). The rats were kept under standard conditions of the Conventional Animal Facility at the ICG SB RAS (Novosibirsk, Russia), as described elsewhere [64,74,232]. The total number of rats was 22 (11 aggressive and 11 tame ones), each four months old and weighing 250–270 g, all from different unrelated litters. All the rats were decapitated. Using a handbook technique [233], we excised samples of the hippocampus, which were then flash-frozen in liquid nitrogen and stored at −70 °C until use. Every effort was made to minimize the number of animals under study and to prevent their suffering. This work was conducted in accordance with the guidelines of the Declaration of Helsinki, Directive 2010/63/EU of the European Parliament, and of the European Council resolution of 22 September 2010.

The research protocol was approved by the Interinstitutional Commission on Bioethics at the ICG SB RAS, Novosibirsk, Russia (approval documentation no. 8 dated 19 March 2012).

4.2. RNA-Seq

Total RNA was isolated from ~100 mg of the hippocampus tissue samples of tame (n = 3) and aggressive (n = 3) rats using the TRIzol™ reagent (Invitrogen, Carlsbad, CA, USA). The quality of the total-RNA samples was evaluated using a Bioanalyzer 2100 (Agilent, Santa-Clara, CA, USA). Samples with optimal RNA Integrity Numbers (RINs)

were chosen for further analysis. Additionally, the total RNA was analyzed quantitatively on an Invitrogen Qubit™ 2.0 fluorometer (Invitrogen). Different RNA types were separated with the mirVana™ Kit (Thermo Fisher Scientific, Waltham, MA, USA). The Dynabeads mRNA Purification Kit (Invitrogen) was used to prepare highly purified mRNA from 5 μg of the RNA fraction depleted of small RNAs. Preparation of RNA-seq libraries from 15–30 ng of an mRNA fraction was carried out using the ScriptSeq™ v2 RNA-Seq Library Preparation Kit (epicenter®, Madison, WI, USA). The quality of the obtained libraries was checked on a Bioanalyzer 2100. After normalization, barcoded libraries were pooled and handed over to the Multi-Access Center of Genomic Research (ICG SB RAS, Novosibirsk, Russia) for sequencing on an Illumina NextSeq 550 instrument in a NextSeq® 500/550 High Output Kit v2 cassette (75 cycles) under the assumption of a direct read of 75 nucleotides, with at least 40 million reads.

4.3. Mapping of RNA Sequences to the R. norvegicus Reference Genome

First, the primary raw Fastq files were checked by means of a quality control tool FastQC (https://www.bioinformatics.babraham.ac.uk/projects/fastqc; accessed on 19 December 2018) for high-throughput sequencing data. After that, using the Trimmomatic tool [234], we improved the quality of the raw reads step-by-step as follows: (i) removing a base from either the start or end position if the quality was low, (ii) trimming bases by a sliding-window method, and (iii) removing any remaining reads that were less than 36 bases long. Next, with the help of the TopHat2 toolbox [235], we aligned the trimmed reads to the *R. norvegicus* reference genome (RGSC Rnor_6.0, UCSC version Rn6, July 2014 assembly). Then, in SAMTools version 1.4 [236], we reformatted these alignments into sorted BAM files. After that, using the htseq-count tool from preprocessing software HTSeq v.0.7.2 [237], along with gtf files carrying coordinates of the rat genes according to Rnor_6.0 and an indexed SAM file, we assigned the reads in question to these genes. Finally, in DESeq2 [238] via Web service IRIS (http://bmbl.sdstate.edu/IRIS/; accessed on 16 January 2020), we rated the differential expression of the abovementioned rat genes, and to minimize false-positive error rates, applied Fisher's Z-test [239] with Benjamini's correction for multiple comparisons, as well as discarded all the hypothetical, tentative, predicted, uncharacterized, and protein-non-coding genes.

4.4. qPCR

To selectively and independently verify the tame-versus-aggressive rat hippocampal DEGs found here (Table 2), in this work, we performed a qPCR control assay on the total RNA taken only from the remaining samples of the hypothalamus of tame (n = 8) and aggressive (n = 8) rats. First, with the help of TRIzol™, we isolated total RNA, purified it on Agencourt RNAClean XP Kit magnetic beads (Beckman, #A63987), and quantified it by means of a Qubit™ 2.0 fluorometer (Invitrogen/Life Technologies) along with an RNA High-Sensitivity Kit (Invitrogen, cat. # Q32852). After that, we synthesized cDNA using the Reverse Transcription Kit (Syntol, #OT-1). Next, using web service PrimerBLAST [240], we designed oligonucleotide primers for qPCR (Table 12).

After that, we carried out qPCR on a LightCycler® 96 (Roche, Basel, Basel-Stadt, Switzerland) with the EVA Green I Kit in three technical replicates. We determined the qPCR efficiency by means of serial cDNA dilutions (standards). In line with the commonly accepted recommendations [76], we simultaneously analyzed four reference genes, namely: *B2m* (β-2-microglobulin) [241], *Hprt1* (hypoxanthine phosphoribosyltransferase 1) [242], *Ppia* (peptidylprolyl isomerase A) [243], and *Rpl30* (ribosomal protein L30) [244].

Table 12. qPCR primers selected using publicly available Web service PrimerBLAST [240].

No.	*Gene*	Forward, 5′→3′	Reverse, 5′→3′
DEGs identified in hippocampus of tame versus aggressive adult male rats [this work]			
1	*Ascl3*	CCTCTGCTGCCCTTTTCCAG	ACTTGACTCGCTGCCTCTCT
2	*Defb17*	TGGTAGCTTGGACTTGAGGAAAGAA	TGCAGCAGTGTGTTCCAGGTC
Reference genes			
3	*B2m*	GTGTCTCAGTTCCACCCACC	TTACATGTCTCGGTCCCAGG
4	*Hprt1*	TCCCAGCGTCGTGATTAGTGA	CCTTCATGACATCTCGAGCAAG
5	*Ppia*	TTCCAGGATTCATGTGCCAG	CTTGCCATCCAGCCACTC
6	*Rpl30*	CATCTTGGCGTCTGATCTTG	TCAGAGTCTGTTTGTACCCC

Notes. Regarding the DEGs subjected to this qPCR verification, see Table 2; reference rat genes: *B2m*, β-2-microglobulin [241]; *Hprt1*, hypoxanthine phosphoribosyltransferase 1 [242]; *Ppia*, peptidylprolyl isomerase A [243]; *Rpl30*, ribosomal protein L30 [244].

4.5. DEGs under Study

In this work, we analyzed all the publicly available independent experimental RNA-Seq datasets—on transcriptomes from the tissues of hypertensive versus normotensive patients [26–39], hypertensive versus normotensive animals [7,40–57], and domestic versus wild animals [72,176–193].

4.6. Human Genes under Study

Here, we analyzed the 42 human genes that are orthologous to the 42 hippocampal DEGs of the tame versus aggressive rats (Table 2). Using the PubMed database [69], we characterized each of these 42 human genes in terms of what is already clinically known about how their underexpression or overexpression can manifest itself in hypertension (Table 9 and Tables S3 and S4).

4.7. DNA Sequences under Study

For in silico analysis of the human genes encoding candidate molecular markers for hypertension that were for the first time suggested in this work, we retrieved both DNA sequences and SNPs of their 70 bp proximal promoters from the Ensembl database [209] and from the dbSNP database [210], respectively, relative to reference human genome assembly GRCh38/hg38 using the UCSC Genome Browser [206] in the dialog mode and additionally by means of toolbox BioPerl [207] in the automated mode, as shown in Figure S2.

4.8. In Silico Analysis of DNA Sequences

We examined SNPs within DNA sequences using our previously developed public web service SNP_TATA_Comparator [203], which applies our bioinformatic model of three-step binding between TBP and a human gene promoter, as detailed in the Supplementary Materials (i.e., Section S1 "Supplementary methods for DNA sequence analysis") and additionally exemplified in Figure S2.

4.9. In Vitro Measurements

In this project, we in vitro measured K_D values expressed in "moles per liter" units of the equilibrium dissociation constant of TBP promoter complexes by means of the EMSA, for each of the nine chosen candidate SNP markers for hypertension subjected to this experimental verification—i.e., rs35518301:g, rs34166473:c, rs34500389:t, rs33980857:a, rs34598529:g, rs33931746:g, rs33931746:c, rs281864525:c, and rs63750953:deletion—as described in-depth in the Supplementary Materials (i.e., Section S2 "Supplementary methods for in vitro measurement").

4.10. Knowledge Base on Domestic Animals' DEGs with Orthologous Human Genes that Can Affect Hypertension

In files with the flat Excel-compatible textual format, here, on the one hand, we first documented all the suggested associations between DEGs (of domestic versus wild animals)

homologous to the 42 DEGs (in the hippocampus of tame and aggressive rats) identified in this study. On the other hand, we documented how underexpression or overexpression of the human genes homologous to these hippocampal rat DEGs can affect hypertension. Next, using the MariaDB 10.2.12 web environment (MariaDB Corp AB, Espoo, Finland), we added the current findings to our previously created PetDEGsDB knowledge base, which is publicly available at www.sysbio.ru/domestic-wild (accessed on 16 January 2020).

4.11. Statistical Analysis

Using the options in the standard toolbox of Statistica (Statsoft^{TM}), we applied the Mann–Whitney *U* test, Fisher's Z-test, Pearson's linear correlation test, the Goodman–Kruskal generalized correlation test, Spearman's and Kendall's rank correlation tests, Pearson's χ^2 test, Fisher's exact test, and binomial-distribution analysis.

Besides this, using the PAST4.04 software package [77], we conducted principal component analysis in the Bootstrap-refinement mode via its mode selection path "Multivariate" → "Ordination" → "Principal Components (PCA)" → "Correlation" → "Bootstrap."

5. Conclusions

First of all, in this work, we performed high-throughput sequencing of the hippocampus transcriptome for three tame adult male rats compared with three aggressive ones (all unrelated animals). The primary experimental data are publicly available for those who would like to use them (NCBI SRA database ID: PRJNA668014) [75].

With the help of this transcriptome, we found the 42 hippocampal DEGs—in the tame versus aggressive rats in question—with statistical significance ($P_{ADJ} < 0.05$, Fisher's Z-test with Benjamini's correction for multiple comparisons) that was conventionally acceptable (Table 2). Moreover, we selectively validated these DEGs by independent experimental analyses (qPCR) of the other eight tame versus eight aggressive adult male rats from different unrelated litters of the same two outbred strains (Table 3 and Figure 1).

Besides this, using these 42 hippocampal tame-versus-aggressive rat DEGs, which reflect rat stress reactivity, we meta-analyzed (by homology) all the highly specific DEGs—of hypertensive versus normotensive subjects (i.e., patients and animals)—that we could find within mainstream hypertension-related transcriptomic research articles. First, we found significant correlations between stress reactivity-related and hypertension-related conventional log2 values (fold changes) of the homologous DEGs analyzed. Next, we found principal components, PC1 and PC2, corresponding to a half-difference and half-sum of these log2 values. Finally, these data pointed to downregulation of hemoglobin or β-protocadherins, corresponding to low blood viscosity [199] or a wide vascular inner diameter [200], as two hypertension theranostic molecular markers applicable to everyone, everywhere, anytime.

Supplementary Materials: Supplementary materials can be found at https://www.mdpi.com/article/10.3390/ijms23052835/s1.

Author Contributions: Conceptualization and supervision, N.A.K.; methodology, A.M., M.N., O.R. and N.G.K.; investigation, I.C., R.K., N.V.K. and S.S.; software, A.B.; validation, E.S. and P.P.; resources, D.O.; data curation, K.Z. and B.K.; writing—original draft preparation, M.P. All authors have read and agreed to the published version of the manuscript.

Funding: This study was supported by the Russian Science Foundation (project no. 19-74-10041).

Institutional Review Board Statement: This work was conducted in accordance with the guidelines of the Declaration of Helsinki, Directive 2010/63/EU of the European Parliament, and of the European Council resolution of 22 September 2010. The research protocol was approved by the Interinstitutional Commission on Bioethics at the ICG SB RAS, Novosibirsk, Russia (Approval documentation no. 8 dated 19 March 2012).

Informed Consent Statement: Not applicable.

Data Availability Statement: The primary RNA-Seq data obtained in this work were deposited in the NCBI SRA database (ID = PRJNA668014).

Acknowledgments: We are grateful to Nikolai Shevchuk (Shevchuk Editing Co., Brooklyn, NY, USA) for fruitful discussions of the work and assistance with adapting it to the requirements of the English language for scientific publications. We are also thankful to the Multi-Access Center "Bioinformatics" for the use of computational resources as supported by Russian government project FWNR-2022-0020. We are appreciative of the Center for Genomic Research at the ICG SB RAS, where RNA-Seq was carried out, as supported by the Russian Federal Science and Technology Program for the Development of Genetic Technologies.

Conflicts of Interest: The authors declare no conflict of interest.

Abbreviations

DEG	differentially expressed gene
EMSA	electrophoretic mobility shift assay
HT	hypertension
log2 value	$\log_2$-transformed gene expression fold change
PC1 (PC2)	major (minor) principal component
qPCR	quantitative polymerase chain reaction
RNA-Seq	RNA sequencing
SNP	single-nucleotide polymorphism
TBP	TATA-binding protein

References

1. Alpsoy, S. Exercise and hypertension. *Adv. Exp. Med. Biol.* **2020**, *1228*, 153–167. [PubMed]
2. Barquera, S.; Pedroza-Tobias, A.; Medina, C.; Hernandez-Barrera, L.; Bibbins-Domingo, K.; Lozano, R.; Moran, A.E. Global overview of the epidemiology of atherosclerotic cardiovascular disease. *Arch. Med. Res.* **2015**, *46*, 328–338. [CrossRef] [PubMed]
3. Meade, R.D.; Akerman, A.P.; Notley, S.R.; McGinn, R.; Poirier, P.; Gosselin, P.; Kenny, G.P. Physiological factors characterizing heat-vulnerable older adults: A narrative review. *Environ. Int.* **2020**, *144*, 105909. [CrossRef]
4. Samanic, C.M.; Barbour, K.E.; Liu, Y.; Wang, Y.; Fang, J.; Lu, H.; Schieb, L.; Greenlund, K.J. Prevalence of self-reported hypertension and antihypertensive medication use by county and rural-urban classification-United States, 2017. *MMWR-Morb. Mortal. Wkly. Rep.* **2020**, *69*, 533–539. [CrossRef]
5. Karaduman, M.; Aparci, M.; Unlu, M.; Ozturk, C.; Balta, S.; Celik, T. Role of screening tests in the detection and management of blood pressure abnormalities among young population. *Angiology* **2017**, *68*, 441–446. [CrossRef]
6. Huang, Q.T.; Chen, J.H.; Hang, L.L.; Liu, S.S.; Zhong, M. Activation of PAR-1/NADPH oxidase/ROS signaling pathways is crucial for the thrombin-induced sFlt-1 production in extravillous trophoblasts: Possible involvement in the pathogenesis of preeclampsia. *Cell. Physiol. Biochem.* **2015**, *35*, 1654–1662. [CrossRef]
7. Tharmalingam, S.; Khurana, S.; Murray, A.; Lamothe, J.; Tai, T.C. Whole transcriptome analysis of adrenal glands from prenatal glucocorticoid programmed hypertensive rodents. *Sci. Rep.* **2020**, *10*, 18755. [CrossRef] [PubMed]
8. Mardenkyzy, D.; Rakhimzhanova, R.; Dautov, T.; Jongmin, L.; Saduakasova, A.; Kozhakhmetova, Z.; Yelshibaeyva, E. Possibilities of computer tomography in the diagnosis of pulmonary hypertension and influence of various factors (gender, age, body weight, reception of medicines) on the severity of the pulmonary hypertension syndrome. *Georgian Med. News* **2020**, *303*, 67–72.
9. Khan, A.W.; Olds, G.; Malik, F.; Teran, P.; Hall, N.; Ali, M. Acute myeloid leukemia masquerading as idiopathic intracranial hypertension: A rare initial presentation. *Kans. J. Med.* **2021**, *14*, 133–135. [CrossRef]
10. Adams-Campbell, L.L.; Taylor, T.; Hicks, J.; Lu, J.; Dash, C. The effect of a 6-month exercise intervention trial on allostatic load in black women at increased risk for breast cancer: The FIERCE study. *J. Racial Ethn. Health Disparities* **2021**. [CrossRef] [PubMed]
11. Gilard, V.; Ferey, J.; Marguet, F.; Fontanilles, M.; Ducatez, F.; Pilon, C.; Lesueur, C.; Pereira, T.; Basset, C.; Schmitz-Afonso, I.; et al. Integrative metabolomics reveals deep tissue and systemic metabolic remodeling in glioblastoma. *Cancers* **2021**, *13*, 5157. [CrossRef] [PubMed]
12. Cheng, Y.X.; Peng, D.; Tao, W.; Zhang, W. Effect of oncometabolic surgery on gastric cancer: The remission of hypertension, type 2 diabetes mellitus, and beyond. *World J. Gastrointest. Oncol.* **2021**, *13*, 1157–1163. [CrossRef]
13. Palacios, D.A.; Zabor, E.C.; Munoz-Lopez, C.; Roversi, G.; Mahmood, F.; Abramczyk, E.; Kelly, M.; Wilson, B.; Abouassaly, R.; Campbell, S.C. Does reduced renal function predispose to cancer-specific mortality from renal cell carcinoma? *Eur. Urol.* **2021**, *79*, 774–780. [CrossRef] [PubMed]
14. Qi, X.L. Current status and prospects of clinical research on portal hypertension in China. *Zhonghua Gan Zang Bing Za Zhi (Chin. J. Hepatol.)* **2021**, *29*, 817–819.

15. Saltalamacchia, G.; Frascaroli, M.; Bernardo, A.; Quaquarini, E. Renal and cardiovascular toxicities by new systemic treatments for prostate cancer. *Cancers* **2020**, *12*, 1750. [CrossRef] [PubMed]
16. Gu, D.; Fang, D.; Zhang, M.; Guo, J.; Ren, H.; Li, X.; Zhang, Z.; Yang, D.; Zou, X.; Liu, Y.; et al. Gastrin, via activation of PPARα, protects the kidney against hypertensive injury. *Clin. Sci.* **2021**, *135*, 409–427. [CrossRef]
17. Chou, L.M.; Beyer, M.M.; Butt, K.M.; Manis, T.; Friedman, E.A. Hypertension jeopardizes diabetic patients following renal transplant. *Trans. Am. Soc. Artif. Intern. Organs* **1984**, *30*, 473–478. [PubMed]
18. Yousaf, M.; Ayasse, M.; Ahmed, A.; Gwillim, E.C.; Janmohamed, S.R.; Yousaf, A.; Patel, K.R.; Thyssen, J.P.; Silverberg, J.I. Association between atopic dermatitis and hypertension: A systematic review and meta-analysis. *Br. J. Dermatol.* **2021**. [CrossRef]
19. Lukawski, K.; Czuczwar, S.J. Assessment of drug-drug interactions between moxonidine and antiepileptic drugs in the maximal electroshock seizure test in mice. *Basic Clin. Pharmacol. Toxicol.* **2021**, *130*, 28–34. [CrossRef] [PubMed]
20. Dinc, H.O.; Saltoglu, N.; Can, G.; Balkan, I.I.; Budak, B.; Ozbey, D.; Caglar, B.; Karaali, R.; Mete, B.; Tuyji Tok, Y.; et al. Inactive SARS-CoV-2 vaccine generates high antibody responses in healthcare workers with and without prior infection. *Vaccine* **2022**, *40*, 52–58. [CrossRef] [PubMed]
21. Page, I.H. The Mosaic Theory of arterial hypertension-: Its interpretation. *Perspect. Biol. Med.* **1967**, *10*, 325–333. [CrossRef] [PubMed]
22. Arishe, O.O.; Priviero, F.; Wilczynski, S.A.; Webb, R.C. Exosomes as intercellular messengers in hypertension. *Int. J. Mol. Sci.* **2021**, *22*, 11685. [CrossRef]
23. Turner, A.I.; Smyth, N.; Hall, S.J.; Torres, S.J.; Hussein, M.; Jayasinghe, S.U.; Ball, K.; Clow, A.J. Psychological stress reactivity and future health and disease outcomes: A systematic review of prospective evidence. *Psychoneuroendocrinology* **2020**, *114*, 104599. [CrossRef] [PubMed]
24. Cannon, W.B. The emergency function of the adrenal medulla in pain and the major emotions. *Am. J. Physiol.* **1914**, *33*, 356–372. [CrossRef]
25. Poulter, N.R.; Prabhakaran, D.; Caulfield, M. Hypertension. *Lancet* **2015**, *386*, 801–812. [CrossRef]
26. Wu, Y.B.; Zang, W.D.; Yao, W.Z.; Luo, Y.; Hu, B.; Wang, L.; Liang, Y.L. Analysis of FOS, BTG2, and NR4A in the function of renal medullary hypertension. *Genet. Mol. Res.* **2013**, *12*, 3735–3741. [CrossRef] [PubMed]
27. Qiu, X.; Lin, J.; Liang, B.; Chen, Y.; Liu, G.; Zheng, J. Identification of hub genes and microRNAs associated with idiopathic pulmonary arterial hypertension by integrated bioinformatics analyses. *Front. Genet.* **2021**, *12*, 667406. [CrossRef] [PubMed]
28. Stearman, R.S.; Bui, Q.M.; Speyer, G.; Handen, A.; Cornelius, A.R.; Graham, B.B.; Kim, S.; Mickler, E.A.; Tuder, R.M.; Chan, S.Y.; et al. Systems analysis of the human pulmonary arterial hypertension lung transcriptome. *Am. J. Respir. Cell Mol. Biol.* **2019**, *60*, 637–649. [CrossRef] [PubMed]
29. Li, C.; Zhang, Z.; Xu, Q.; Wu, T.; Shi, R. Potential mechanisms and serum biomarkers involved in sex differences in pulmonary arterial hypertension. *Medicine* **2020**, *99*, e19612. [CrossRef] [PubMed]
30. Yao, X.; Jing, T.; Wang, T.; Gu, C.; Chen, X.; Chen, F.; Feng, H.; Zhao, H.; Chen, D.; Ma, W. Molecular characterization and elucidation of pathways to identify novel therapeutic targets in pulmonary arterial hypertension. *Front. Physiol.* **2021**, *12*, 694702. [CrossRef]
31. Awad, K.S.; Elinoff, J.M.; Wang, S.; Gairhe, S.; Ferreyra, G.A.; Cai, R.; Sun, J.; Solomon, M.A.; Danner, R.L. Raf/ERK drives the proliferative and invasive phenotype of BMPR2-silenced pulmonary artery endothelial cells. *Am. J. Physiol. Lung Cell. Mol. Physiol.* **2016**, *310*, L187–L201. [CrossRef]
32. Saei, H.; Govahi, A.; Abiri, A.; Eghbali, M.; Abiri, M. Comprehensive transcriptome mining identified the gene expression signature and differentially regulated pathways of the late-onset preeclampsia. *Pregnancy Hypertens.* **2021**, *25*, 91–102. [CrossRef] [PubMed]
33. Jung, Y.W.; Shim, J.I.; Shim, S.H.; Shin, Y.J.; Shim, S.H.; Chang, S.W.; Cha, D.H. Global gene expression analysis of cell-free RNA in amniotic fluid from women destined to develop preeclampsia. *Medicine* **2019**, *98*, e13971. [CrossRef] [PubMed]
34. Textoris, J.; Ivorra, D.; Ben Amara, A.; Sabatier, F.; Menard, J.P.; Heckenroth, H.; Bretelle, F.; Mege, J.L. Evaluation of current and new biomarkers in severe preeclampsia: A microarray approach reveals the VSIG4 gene as a potential blood biomarker. *PLoS ONE* **2013**, *8*, e82638. [CrossRef]
35. Yong, H.E.; Melton, P.E.; Johnson, M.P.; Freed, K.A.; Kalionis, B.; Murthi, P.; Brennecke, S.P.; Keogh, R.J.; Moses, E.K. Genome-wide transcriptome directed pathway analysis of maternal pre-eclampsia susceptibility genes. *PLoS ONE* **2015**, *10*, e0128230. [CrossRef] [PubMed]
36. Ahn, S.; Jeong, E.; Min, J.W.; Kim, E.; Choi, S.S.; Kim, C.J.; Lee, D.C. Identification of genes dysregulated by elevation of microRNA-210 levels in human trophoblasts cell line, Swan 71. *Am. J. Reprod. Immunol.* **2017**, *78*, e12722. [CrossRef]
37. Neusser, M.A.; Lindenmeyer, M.T.; Moll, A.G.; Segerer, S.; Edenhofer, I.; Sen, K.; Stiehl, D.P.; Kretzler, M.; Grone, H.J.; Schlondorff, D.; et al. Human nephrosclerosis triggers a hypoxia-related glomerulopathy. *Am. J. Pathol.* **2010**, *176*, 594–607. [CrossRef] [PubMed]
38. Koper, A.; Zeef, L.A.; Joseph, L.; Kerr, K.; Gosney, J.; Lindsay, M.A.; Booton, R. Whole transcriptome analysis of pre-invasive and invasive early squamous lung carcinoma in archival laser microdissected samples. *Respir. Res.* **2017**, *18*, 12. [CrossRef] [PubMed]
39. Zheng, Y.; He, J.Q. Common differentially expressed genes and pathways correlating both coronary artery disease and atrial fibrillation. *EXCLI J.* **2021**, *20*, 126–141.

40. Stefanova, N.A.; Maksimova, K.Y.; Rudnitskaya, E.A.; Muraleva, N.A.; Kolosova, N.G. Association of cerebrovascular dysfunction with the development of Alzheimer's disease-like pathology in OXYS rats. *BMC Genom.* **2018**, *19*, 75. [CrossRef] [PubMed]
41. Stefanova, N.A.; Ershov, N.I.; Maksimova, K.Y.; Muraleva, N.A.; Tyumentsev, M.A.; Kolosova, N.G. The rat prefrontal-cortex transcriptome: Effects of aging and sporadic Alzheimer's disease-like pathology. *J. Gerontol. A Biol. Sci. Med. Sci.* **2019**, *74*, 33–43. [CrossRef]
42. Kozhevnikova, O.S.; Korbolina, E.E.; Ershov, N.I.; Kolosova, N.G. Rat retinal transcriptome: Effects of aging and AMD-like retinopathy. *Cell Cycle* **2013**, *12*, 1745–1761. [CrossRef]
43. Fedoseeva, L.A.; Klimov, L.O.; Ershov, N.I.; Efimov, V.M.; Markel, A.L.; Orlov, Y.L.; Redina, O.E. The differences in brain stem transcriptional profiling in hypertensive ISIAH and normotensive WAG rats. *BMC Genom.* **2019**, *20*, 297. [CrossRef]
44. Klimov, L.O.; Ershov, N.I.; Efimov, V.M.; Markel, A.L.; Redina, O.E. Genome-wide transcriptome analysis of hypothalamus in rats with inherited stress-induced arterial hypertension. *BMC Genet.* **2016**, *17*, 13. [CrossRef]
45. Ryazanova, M.A.; Fedoseeva, L.A.; Ershov, N.I.; Efimov, V.M.; Markel, A.L.; Redina, O.E. The gene-expression profile of renal medulla in ISIAH rats with inherited stress-induced arterial hypertension. *BMC Genet.* **2016**, *17* (Suppl. S3), 151. [CrossRef]
46. Fedoseeva, L.A.; Ryazanova, M.A.; Ershov, N.I.; Markel, A.L.; Redina, O.E. Comparative transcriptional profiling of renal cortex in rats with inherited stress-induced arterial hypertension and normotensive Wistar Albino Glaxo rats. *BMC Genet.* **2016**, *17* (Suppl. S1), 12. [CrossRef] [PubMed]
47. Fedoseeva, L.A.; Klimov, L.O.; Ershov, N.I.; Alexandrovich, Y.V.; Efimov, V.M.; Markel, A.L.; Redina, O.E. Molecular determinants of the adrenal gland functioning related to stress-sensitive hypertension in ISIAH rats. *BMC Genom.* **2016**, *17*, 989. [CrossRef] [PubMed]
48. Yuan, X.; Wu, Q.; Liu, X.; Zhang, H.; Xiu, R. Transcriptomic profile analysis of brain microvascular pericytes in spontaneously hypertensive rats by RNA-Seq. *Am. J. Transl. Res.* **2018**, *10*, 2372–2386. [PubMed]
49. Watanabe, Y.; Yoshida, M.; Yamanishi, K.; Yamamoto, H.; Okuzaki, D.; Nojima, H.; Yasunaga, T.; Okamura, H.; Matsunaga, H.; Yamanishi, H. Genetic analysis of genes causing hypertension and stroke in spontaneously hypertensive rats: Gene expression profiles in the kidneys. *Int. J. Mol. Med.* **2015**, *36*, 712–724. [CrossRef] [PubMed]
50. Xiao, G.; Wang, T.; Zhuang, W.; Ye, C.; Luo, L.; Wang, H.; Lian, G.; Xie, L. RNA sequencing analysis of monocrotaline-induced PAH reveals dysregulated chemokine and neuroactive ligand receptor pathways. *Aging* **2020**, *12*, 4953–4969. [CrossRef] [PubMed]
51. Du, H.; Xiao, G.; Xue, Z.; Li, Z.; He, S.; Du, X.; Zhou, Z.; Cao, L.; Wang, Y.; Yang, J.; et al. QiShenYiQi ameliorates salt-induced hypertensive nephropathy by balancing ADRA1D and SIK1 expression in Dahl salt-sensitive rats. *Biomed. Pharmacother.* **2021**, *141*, 111941. [CrossRef] [PubMed]
52. Ashraf, U.M.; Mell, B.; Jose, P.A.; Kumarasamy, S. Deep transcriptomic profiling of Dahl salt-sensitive rat kidneys with mutant form of Resp18. *Biochem. Biophys. Res. Commun.* **2021**, *572*, 35–40. [CrossRef] [PubMed]
53. Zhou, X.; Zhang, X.X.; Mahmmod, Y.S.; Hernandez, J.A.; Li, G.F.; Huang, W.Y.; Wang, Y.P.; Zheng, Y.X.; Li, X.M.; Yuan, Z.G. A Transcriptome analysis: Various reasons of adverse pregnancy outcomes caused by acute toxoplasma gondii infection. *Front. Physiol.* **2020**, *11*, 115. [CrossRef]
54. Puig, O.; Wang, I.M.; Cheng, P.; Zhou, P.; Roy, S.; Cully, D.; Peters, M.; Benita, Y.; Thompson, J.; Cai, T.Q. Transcriptome profiling and network analysis of genetically hypertensive mice identifies potential pharmacological targets of hypertension. *Physiol. Genom.* **2010**, *42A*, 24–32. [CrossRef] [PubMed]
55. Loke, S.Y.; Wong, P.T.; Ong, W.Y. Global gene expression changes in the prefrontal cortex of rabbits with hypercholesterolemia and/or hypertension. *Neurochem. Int.* **2017**, *102*, 33–56. [CrossRef] [PubMed]
56. Park, W.; Rengaraj, D.; Kil, D.Y.; Kim, H.; Lee, H.K.; Song, K.D. RNA-seq analysis of the kidneys of broiler chickens fed diets containing different concentrations of calcium. *Sci. Rep.* **2017**, *7*, 11740. [CrossRef]
57. Yang, F.; Cao, H.; Xiao, Q.; Guo, X.; Zhuang, Y.; Zhang, C.; Wang, T.; Lin, H.; Song, Y.; Hu, G.; et al. Transcriptome analysis and gene identification in the pulmonary artery of broilers with ascites syndrome. *PLoS ONE* **2016**, *11*, e0156045. [CrossRef] [PubMed]
58. Trovato, G.M. Sustainable medical research by effective and comprehensive medical skills: Overcoming the frontiers by predictive, preventive and personalized medicine. *EPMA J.* **2014**, *5*, 14. [CrossRef] [PubMed]
59. Osadchuk, A.V.; Markel, A.L.; Khusainov, R.A.; Naumenko, E.V.; Beliaev, D.K. Problems in the genetics of stress. IV. A genetic analysis of the level of autonomic reactivity in emotional stress in rats. *Sov. Genet.* **1979**, *15*, 1847–1857.
60. Markel, A.L. Features of the behavior of the rat with hereditarily determined arterial hypertension. *Zhurnal Vyss. Nervn. Deiatelnosti Im. IP Pavlov.* **1986**, *36*, 956–962.
61. Herbek, Y.E.; Zakharov, I.K.; Trapezov, O.V.; Shumny, V.K. Evolution compressed in time. *Philos. Sci.* **2013**, *1*, 115–139.
62. Oskina, I.N.; Herbeck, Y.E.; Shikhevich, S.G.; Plyusnina, I.Z.; Gulevich, R.G. Alterations in the hypothalamus-pituitary-adrenal and immune systems during selection of animals for tame behavior. *Inf. Bull. VOGiS* **2008**, *12*, 39–49.
63. Prasolova, L.A.; Gerbek, Y.E.; Gulevich, R.G.; Shikhevich, S.G.; Konoshenko, M.Y.; Kozhemyakina, R.V.; Oskina, I.N.; Plyusnina, I.Z. The effects of prolonged selection for behavior on the stress response and activity of the reproductive system of male grey mice (Rattus norvegicus). *Russ. J. Genet.* **2014**, *50*, 846–852. [CrossRef]
64. Belyaev, D.K.; Borodin, P.M. The influence of stress on variation and its role in evolution. *Biol. Zent.* **1982**, *100*, 705–714.
65. Kolosova, N.G.; Stefanova, N.A.; Korbolina, E.E.; Fursova, A.Z.; Kozhevnikova, O.S. Senescence-accelerated OXYS rats: A genetic model of premature aging and age-related diseases. *Adv. Gerontol.* **2014**, *27*, 336–340. [CrossRef]

66. Stefanova, N.A.; Kozhevnikova, O.S.; Vitovtov, A.O.; Maksimova, K.Y.; Logvinov, S.V.; Rudnitskaya, E.A.; Korbolina, E.E.; Muraleva, N.A.; Kolosova, N.G. Senescence-accelerated OXYS rats: A model of age-related cognitive decline with relevance to abnormalities in Alzheimer disease. *Cell Cycle* **2014**, *13*, 898–909. [CrossRef] [PubMed]
67. Devyatkin, V.A.; Redina, O.E.; Muraleva, N.A.; Kolosova, N.G. Single-nucleotide polymorphisms (SNPs) both associated with hypertension and contributing to accelerated-senescence traits in OXYS rats. *Int. J. Mol. Sci.* **2020**, *21*, 3542. [CrossRef] [PubMed]
68. Devyatkin, V.A.; Redina, O.E.; Kolosova, N.G.; Muraleva, N.A. Single-nucleotide polymorphisms associated with the senescence-accelerated phenotype of OXYS rats: A focus on Alzheimer's disease-like and age-related-macular-degeneration-like pathologies. *J. Alzheimer's Dis.* **2020**, *73*, 1167–1183. [CrossRef] [PubMed]
69. Lu, Z. PubMed and beyond: A survey of web tools for searching biomedical literature. *Database* **2011**, *2011*, baq036. [CrossRef] [PubMed]
70. Vasiliev, G.; Chadaeva, I.; Rasskazov, D.; Ponomarenko, P.; Sharypova, E.; Drachkova, I.; Bogomolov, A.; Savinkova, L.; Ponomarenko, M.; Kolchanov, N.; et al. A bioinformatics model of human diseases on the basis of differentially expressed genes (of domestic versus wild animals) that are orthologs of human genes associated with reproductive-potential changes. *Int. J. Mol. Sci.* **2021**, *22*, 2346. [CrossRef] [PubMed]
71. Klimova, N.V.; Oshchepkova, E.; Chadaeva, I.; Sharypova, E.; Ponomarenko, P.; Drachkova, I.; Rasskazov, D.; Oshchepkov, D.; Ponomarenko, M.; Savinkova, L.; et al. Disruptive selection of human immunostimulatory and immunosuppressive genes both provokes and prevents rheumatoid arthritis, respectively, as a self-domestication syndrome. *Front. Genet.* **2021**, *12*, 610774. [CrossRef] [PubMed]
72. Chadaeva, I.; Ponomarenko, P.; Kozhemyakina, R.; Suslov, V.; Bogomolov, A.; Klimova, N.; Shikhevich, S.; Savinkova, L.; Oshchepkov, D.; Kolchanov, N.A.; et al. Domestication explains two-thirds of differential-gene-expression variance between domestic and wild animals; the remaining one-third reflects intraspecific and interspecific variation. *Animals* **2021**, *11*, 2667. [CrossRef] [PubMed]
73. Hecht, K.; Hai, N.V.; Hecht, T.; Moritz, V.; Woossmann, H. Correlations between hippocampus function and stressed learning and their effect on cerebro-visceral regulation processes. *Acta Biol. Med. Ger.* **1976**, *35*, 35–45. [PubMed]
74. Plyusnina, I.; Oskina, I. Behavioral and adrenocortical responses to open-field test in rats selected for reduced aggressiveness toward humans. *Physiol. Behav.* **1997**, *61*, 381–385. [CrossRef]
75. Sayers, E.W.; Beck, J.; Bolton, E.E.; Bourexis, D.; Brister, J.R.; Canese, K.; Comeau, D.C.; Funk, K.; Kim, S.; Klimke, W.; et al. Database resources of the National Center for Biotechnology Information. *Nucleic Acids Res.* **2021**, *49*, D10–D17. [CrossRef]
76. Bustin, S.A.; Benes, V.; Garson, J.A.; Hellemans, J.; Huggett, J.; Kubista, M.; Mueller, R.; Nolan, T.; Pfaffl, M.W.; Shipley, G.L.; et al. The MIQE guidelines: Minimum information for publication of quantitative real-time PCR experiments. *Clin. Chem.* **2009**, *55*, 611–622. [CrossRef] [PubMed]
77. Hammer, O.; Harper, D.A.T.; Ryan, P.D. PAST: Paleontological statistics software package for education and data analysis. *Palaeontol. Electron.* **2001**, *4*, 1–9.
78. McNeil, J.B.; Jackson, K.E.; Wang, C.; Siew, E.D.; Vincz, A.J.; Shaver, C.M.; Bastarache, J.A.; Ware, L.B. Linear association between hypoalbuminemia and increased risk of acute respiratory distress syndrome in critically ill adults. *Crit Care Explor.* **2021**, *3*, e0527. [CrossRef]
79. Facciorusso, A.; Nacchiero, M.C.; Rosania, R.; Laonigro, G.; Longo, N.; Panella, C.; Ierardi, E. The use of human albumin for the treatment of ascites in patients with liver cirrhosis: Item of safety, facts, controversies and perspectives. *Curr. Drug Saf.* **2011**, *6*, 267–274. [CrossRef] [PubMed]
80. Vassiliou, A.G.; Keskinidou, C.; Kotanidou, A.; Frantzeskaki, F.; Dimopoulou, I.; Langleben, D.; Orfanos, S.E. Knockdown of bone morphogenetic protein type II receptor leads to decreased aquaporin 1 expression and function in human pulmonary microvascular endothelial cells. *Can. J. Physiol. Pharmacol.* **2020**, *98*, 834–839. [CrossRef] [PubMed]
81. Schuoler, C.; Haider, T.J.; Leuenberger, C.; Vogel, J.; Ostergaard, L.; Kwapiszewska, G.; Kohler, M.; Gassmann, M.; Huber, L.C.; Brock, M. Aquaporin 1 controls the functional phenotype of pulmonary smooth muscle cells in hypoxia-induced pulmonary hypertension. *Basic Res. Cardiol.* **2017**, *112*, 30. [CrossRef] [PubMed]
82. Wang, C.Y.; Shahi, P.; Huang, J.T.; Phan, N.N.; Sun, Z.; Lin, Y.C.; Lai, M.D.; Werb, Z. Systematic analysis of the achaete-scute complex-like gene signature in clinical cancer patients. *Mol. Clin. Oncol.* **2017**, *6*, 7–18. [CrossRef] [PubMed]
83. Martin, T.G.; Tawfik, S.; Moravec, C.S.; Pak, T.R.; Kirk, J.A. BAG3 expression and sarcomere localization in the human heart are linked to HSF-1 and are differentially affected by sex and disease. *Am. J. Physiol. Heart Circ. Physiol.* **2021**, *320*, H2339–H2350. [CrossRef] [PubMed]
84. Derosa, G.; Maffioli, P.; Rosati, A.; Basile, A.; D'Angelo, A.; Romano, D.; Sahebkar, A.; Falco, A.; Turco, M.C. Evaluation of BAG3 levels in healthy subjects, hypertensive patients, and hypertensive diabetic patients. *J. Cell. Physiol.* **2018**, *3*, 1791–1795. [CrossRef]
85. Wang, Y.P.; Huang, L.Y.; Sun, W.M.; Zhang, Z.Z.; Fang, J.Z.; Wei, B.F.; Wu, B.H.; Han, Z.G. Insulin receptor tyrosine kinase substrate activates EGFR/ERK signalling pathway and promotes cell proliferation of hepatocellular carcinoma. *Cancer Lett.* **2013**, *337*, 96–106. [CrossRef] [PubMed]
86. Park, J.S.; Pierorazio, P.M.; Lee, J.H.; Lee, H.J.; Lim, Y.S.; Jang, W.S.; Kim, J.; Lee, S.H.; Rha, K.H.; Cho, N.H.; et al. Gene expression analysis of aggressive clinical T1 stage clear cell renal cell carcinoma for identifying potential diagnostic and prognostic biomarkers. *Cancers* **2020**, *12*, 222. [CrossRef]

87. Stojanovic, M.; Goldner, B.; Ivkovic, D. Renal cell carcinoma and arterial hypertension. *Clin. Exp. Nephrol.* **2009**, *13*, 295–299. [CrossRef]
88. Han, F.; Zhao, H.; Lu, J.; Yun, W.; Yang, L.; Lou, Y.; Su, D.; Chen, X.; Zhang, S.; Jin, H.; et al. Anti-Tumor effects of BDH1 in acute myeloid leukemia. *Front. Oncol.* **2021**, *11*, 694594. [CrossRef]
89. Camerino, M.; Giacobino, D.; Manassero, L.; Iussich, S.; Riccardo, F.; Cavallo, F.; Tarone, L.; Olimpo, M.; Lardone, E.; Martano, M.; et al. Prognostic impact of bone invasion in canine oral malignant melanoma treated by surgery and anti-CSPG4 vaccination: A retrospective study on 68 cases (2010–2020). *Vet. Comp. Oncol.* **2021**, *20*, 189–197. [CrossRef]
90. El-Qushayri, A.E.; Benmelouka, A.Y.; Salman, S.; Nardone, B. Melanoma and hypertension, is there an association? A U.S. population based study. *Ital. J. Dermatol. Venerol.* **2021**. [CrossRef]
91. Damour, A.; Garcia, M.; Seneschal, J.; Leveque, N.; Bodet, C. Eczema herpeticum: Clinical and pathophysiological aspects. *Clin. Rev. Allergy Immunol.* **2020**, *59*, 1–18. [CrossRef] [PubMed]
92. Ohtani, M.; Nishimura, T. Sulfur-containing amino acids in aged garlic extract inhibit inflammation in human gingival epithelial cells by suppressing intercellular adhesion molecule-1 expression and IL-6 secretion. *Biomed. Rep.* **2020**, *12*, 99–108. [CrossRef] [PubMed]
93. Liu, R.; Zhang, Z.; Liu, H.; Hou, P.; Lang, J.; Wang, S.; Yan, H.; Li, P.; Huang, Z.; Wu, H.; et al. Human β-defensin 2 is a novel opener of Ca2+-activated potassium channels and induces vasodilation and hypotension in monkeys. *Hypertension* **2013**, *62*, 415–425. [CrossRef] [PubMed]
94. He, L.; Yang, Y.; Chen, J.; Zou, P.; Li, J. Transcriptional activation of ENPP2 by FoxO4 protects cardiomyocytes from doxorubicin-induced toxicity. *Mol. Med. Rep.* **2021**, *24*, 668. [CrossRef]
95. Matsumura, N.; Zordoky, B.N.; Robertson, I.M.; Hamza, S.M.; Parajuli, N.; Soltys, C.M.; Beker, D.L.; Grant, M.K.; Razzoli, M.; Bartolomucci, A.; et al. Co-administration of resveratrol with doxorubicin in young mice attenuates detrimental late-occurring cardiovascular changes. *Cardiovasc. Res.* **2018**, *114*, 1350–1359. [CrossRef] [PubMed]
96. Xu, X.Y.; Guo, W.J.; Pan, S.H.; Zhang, Y.; Gao, F.L.; Wang, J.T.; Zhang, S.; Li, H.Y.; Wang, R.; Zhang, X. TILRR (FREM1 isoform 2) is a prognostic biomarker correlated with immune infiltration in breast cancer. *Aging* **2020**, *12*, 19335–19351. [CrossRef]
97. Li, H.N.; Li, X.R.; Lv, Z.T.; Cai, M.M.; Wang, G.; Yang, Z.F. Elevated expression of FREM1 in breast cancer indicates favorable prognosis and high-level immune infiltration status. *Cancer Med.* **2020**, *9*, 9554–9570. [CrossRef]
98. Wang, S.; Zhu, G.; Jiang, D.; Rhen, J.; Li, X.; Liu, H.; Lyu, Y.; Tsai, P.; Rose, Y.; Nguyen, T.; et al. Reduced Notch1 cleavage promotes the development of pulmonary hypertension. *Hypertension* **2021**, *79*, 79–92. [CrossRef]
99. Zhou, C.; Yu, J.; Wang, M.; Yang, J.; Xiong, H.; Huang, H.; Wu, D.; Hu, S.; Wang, Y.; Chen, X.Z.; et al. Identification of glycerol-3-phosphate dehydrogenase 1 as a tumour suppressor in human breast cancer. *Oncotarget* **2017**, *8*, 101309–101324. [CrossRef]
100. Azad, G.K.; Singh, V.; Thakare, M.J.; Baranwal, S.; Tomar, R.S. Mitogen-activated protein kinase Hog1 is activated in response to curcumin exposure in the budding yeast Saccharomyces cerevisiae. *BMC Microbiol.* **2014**, *14*, 317. [CrossRef]
101. Kim, Y.B.; Kim, Y.S.; Kim, W.B.; Shen, F.Y.; Lee, S.W.; Chung, H.J.; Kim, J.S.; Han, H.C.; Colwell, C.S.; Kim, Y.I. GABAergic excitation of vasopressin neurons: Possible mechanism underlying sodium-dependent hypertension. *Circ. Res.* **2013**, *113*, 1296–1307. [CrossRef]
102. Triantafyllou, A.I.; Vyssoulis, G.P.; Karpanou, E.A.; Karkalousos, P.L.; Triantafyllou, E.A.; Aessopos, A.; Farmakis, D.T. Impact of β-thalassemia trait carrier state on cardiovascular risk factors and metabolic profile in patients with newly diagnosed hypertension. *J. Hum. Hypertens.* **2014**, *28*, 328–332. [CrossRef] [PubMed]
103. Zheng, H.; Wei, X.C.; Yu, T.; Lei, Q. Anesthesia of a high-altitude area inhabitant who underwent aortic dissection emergency surgery in a low-altitude area. *J. Int. Med. Res.* **2020**, *48*, 300060520979871. [CrossRef] [PubMed]
104. Chen, M.; Li, M.H.; Zhang, N.; Sun, W.W.; Wang, H.; Wang, Y.A.; Zhao, Y.; Wei, W. Pro-angiogenic effect of exosomal microRNA-103a in mice with rheumatoid arthritis via the downregulation of hepatocyte nuclear factor 4 alpha and activation of the JAK/STAT3 signaling pathway. *J. Biol. Regul. Homeost Agents* **2021**, *35*, 629–640. [PubMed]
105. Argnani, L.; Zanetti, A.; Carrara, G.; Silvagni, E.; Guerrini, G.; Zambon, A.; Scire, C.A. Rheumatoid arthritis and cardiovascular risk: Retrospective matched-cohort analysis based on the RECORD study of the italian society for rheumatology. *Front. Med.* **2021**, *8*, 745601. [CrossRef] [PubMed]
106. Ni, Z.; Lu, W.; Li, Q.; Han, C.; Yuan, T.; Sun, N.; Shi, Y. Analysis of the HNF4A isoform-regulated transcriptome identifies CCL15 as a downstream target in gastric carcinogenesis. *Cancer Biol. Med.* **2021**, *18*, 530–546. [CrossRef] [PubMed]
107. Sejourne, J.; Llaneza, D.; Kuti, O.J.; Page, D.T. Social behavioral deficits coincide with the onset of seizure susceptibility in mice lacking serotonin receptor 2c. *PLoS ONE* **2015**, *10*, e0136494. [CrossRef] [PubMed]
108. Veeramachaneni, G.K.; Thunuguntla, V.B.S.C.; Bhaswant, M.; Mathai, M.L.; Bondili, J.S. Pharmacophore directed screening of agonistic natural molecules showing affinity to 5HT2C receptor. *Biomolecules* **2019**, *9*, 556. [CrossRef] [PubMed]
109. Kelm-Nelson, C.A.; Gammie, S. Gene expression within the periaqueductal gray is linked to vocal behavior and early-onset parkinsonism in Pink1 knockout rats. *BMC Genom.* **2020**, *21*, 625. [CrossRef]
110. Shin, N.Y.; Park, Y.W.; Yoo, S.W.; Yoo, J.Y.; Choi, Y.; Jang, J.; Ahn, K.J.; Kim, B.S.; Kim, J.S. Adverse effects of hypertension, supine hypertension, and perivascular space on cognition and motor function in PD. *NPJ Parkinsons Dis.* **2021**, *7*, 69. [CrossRef] [PubMed]

111. Zhao, Z.L.; Du, S.; Shen, S.X.; Luo, P.; Ding, S.K.; Wang, G.G.; Wang, L.X. Biomarkers screening for viral myocarditis through proteomics analysis of plasma exosomes. *Zhonghua Yi Xue Za Zhi (Chin. Med. J.)* **2019**, *99*, 343–348.
112. Fox, S.E.; Falgout, L.; Vander Heide, R.S. COVID-19 myocarditis: Quantitative analysis of the inflammatory infiltrate and a proposed mechanism. *Cardiovasc. Pathol.* **2021**, *54*, 107361. [CrossRef] [PubMed]
113. Karo-Atar, D.; Moshkovits, I.; Eickelberg, O.; Konigshoff, M.; Munitz, A. Paired immunoglobulin-like receptor-B inhibits pulmonary fibrosis by suppressing profibrogenic properties of alveolar macrophages. *Am. J. Respir. Cell Mol. Biol.* **2013**, *48*, 456–464. [CrossRef] [PubMed]
114. Huang, J.; Burke, P.S.; Cung, T.D.; Pereyra, F.; Toth, I.; Walker, B.D.; Borges, L.; Lichterfeld, M.; Yu, X.G. Leukocyte immunoglobulin-like receptors maintain unique antigen-presenting properties of circulating myeloid dendritic cells in HIV-1-infected elite controllers. *J. Virol.* **2010**, *84*, 9463–9471. [CrossRef]
115. Kumar, A.; Mahajan, A.; Salazar, E.A.; Pruitt, K.; Guzman, C.A.; Clauss, M.A.; Almodovar, S.; Dhillon, N.K. Impact of human immunodeficiency virus on pulmonary vascular disease. *Glob. Cardiol. Sci. Pract.* **2021**, *2021*, e202112. [CrossRef]
116. Sakamoto, S.; Matsuura, K.; Masuda, S.; Hagiwara, N.; Shimizu, T. Heart-derived fibroblasts express LYPD-1 and negatively regulate angiogenesis in rat. *Regen. Ther.* **2020**, *15*, 27–33. [CrossRef]
117. Kumar, N.; Verma, R.; Lohana, P.; Lohana, A.; Ramphul, K. Acute myocardial infarction in COVID-19 patients. A review of cases in the literature. *Arch. Med. Sci. Atheroscler Dis.* **2021**, *6*, e169–e175. [CrossRef]
118. Matsushita, Y.; Furukawa, T.; Kasanuki, H.; Nishibatake, M.; Kurihara, Y.; Ikeda, A.; Kamatani, N.; Takeshima, H.; Matsuoka, R. Mutation of junctophilin type 2 associated with hypertrophic cardiomyopathy. *J. Hum. Genet.* **2007**, *52*, 543–548. [CrossRef]
119. Sridharan, A.; Maron, M.S.; Carrick, R.T.; Madias, C.A.; Huang, D.; Cooper, C.; Drummond, J.; Maron, B.J.; Rowin, E.J. Impact of comorbidities on atrial fibrillation and sudden cardiac death in hypertrophic cardiomyopathy. *J. Cardiovasc. Electrophysiol.* **2021**, *33*, 20–29. [CrossRef]
120. Rozanski, A.; Takano, A.P.; Kato, P.N.; Soares, A.G.; Lellis-Santos, C.; Campos, J.C.; Ferreira, J.C.; Barreto-Chaves, M.L.; Moriscot, A.S. M-protein is down-regulated in cardiac hypertrophy driven by thyroid hormone in rats. *Mol. Endocrinol.* **2013**, *27*, 2055–2065. [CrossRef] [PubMed]
121. Grabowski, K.; Herlan, L.; Witten, A.; Qadri, F.; Eisenreich, A.; Lindner, D.; Schadlich, M.; Schulz, A.; Subrova, J.; Mhatre, K.N.; et al. Cpxm2 as a novel candidate for cardiac hypertrophy and failure in hypertension. *Hypertens. Res.* **2021**, *45*, 292–307. [CrossRef] [PubMed]
122. Zeng, Y.; Du, X.; Yao, X.; Qiu, Y.; Jiang, W.; Shen, J.; Li, L.; Liu, X. Mechanism of cell death of endothelial cells regulated by mechanical forces. *J. Biomech.* **2021**, *131*, 110917. [CrossRef] [PubMed]
123. Ashton, K.J.; Tupicoff, A.; Williams-Pritchard, G.; Kiessling, C.J.; See Hoe, L.E.; Headrick, J.P.; Peart, J.N. Unique transcriptional profile of sustained ligand-activated preconditioning in pre- and post-ischemic myocardium. *PLoS ONE* **2013**, *8*, e72278. [CrossRef] [PubMed]
124. Sekino, Y.; Oue, N.; Mukai, S.; Shigematsu, Y.; Goto, K.; Sakamoto, N.; Sentani, K.; Hayashi, T.; Teishima, J.; Matsubara, A.; et al. Protocadherin B9 promotes resistance to bicalutamide and is associated with the survival of prostate cancer patients. *Prostate* **2019**, *79*, 234–242. [CrossRef]
125. Gabbert, L.; Dilling, C.; Meybohm, P.; Burek, M. Deletion of protocadherin gamma C3 induces phenotypic and functional changes in brain microvascular endothelial cells in vitro. *Front. Pharmacol.* **2020**, *11*, 590144. [CrossRef]
126. Wang, H.L.; Zhang, C.L.; Qiu, Y.M.; Chen, A.Q.; Li, Y.N.; Hu, B. Dysfunction of the blood-brain barrier in cerebral microbleeds: From bedside to bench. *Aging Dis.* **2021**, *12*, 1898–1919. [CrossRef]
127. Du, J.; Dong, Y.; Li, Y. Identification and prognostic value exploration of cyclophosphamide (cytoxan)-centered chemotherapy response-associated genes in breast cancer. *DNA Cell Biol.* **2021**, *40*, 1356–1368. [CrossRef]
128. Bloodgood, D.W.; Hardaway, J.A.; Stanhope, C.M.; Pati, D.; Pina, M.M.; Neira, S.; Desai, S.; Boyt, K.M.; Palmiter, R.D.; Kash, T.L. Kappa opioid receptor and dynorphin signaling in the central amygdala regulates alcohol intake. *Mol. Psychiatry* **2021**, *26*, 2187–2199. [CrossRef]
129. Uchiyama, M.; Mizukami, S.; Arima, K.; Nishimura, T.; Tomita, Y.; Abe, Y.; Tanaka, N.; Honda, Y.; Goto, H.; Hasegawa, M.; et al. Association between serum 25-hydroxyvitamin D and physical performance measures in middle-aged and old Japanese men and women: The Unzen study. *PLoS ONE* **2021**, *16*, e0261639. [CrossRef]
130. Landrum, M.; Lee, J.; Riley, G.; Jang, W.; Rubinstein, W.; Church, D.; Maglott, D. ClinVar: Public archive of relationships among sequence variation and human phenotype. *Nucleic Acids Res.* **2014**, *42*, D980–D985. [CrossRef]
131. Elavarasi, A.; Dash, D.; Tripathi, M.; Bhatia, R. Cerebellar ataxia and neuropathy as presenting features of hepatitis-B related cirrhosis and portal hypertension. *BMJ Case Rep.* **2017**, *2017*, bcr2017221912. [CrossRef]
132. Miki, Y.; Kidoguchi, Y.; Sato, M.; Taketomi, Y.; Taya, C.; Muramatsu, K.; Gelb, M.H.; Yamamoto, K.; Murakami, M. Dual roles of group iid phospholipase A2 in inflammation and cancer. *J. Biol. Chem.* **2016**, *291*, 15588–155601. [CrossRef] [PubMed]
133. Karpinska-Mirecka, A.; Bartosinska, J.; Krasowska, D. The impact of hypertension, diabetes, lipid disorders, overweight/obesity and nicotine dependence on health-related quality of life and psoriasis severity in psoriatic patients receiving systemic conventional and biological treatment. *Int. J. Environ. Res. Public Health* **2021**, *18*, 13167. [CrossRef] [PubMed]
134. Htwe, Y.M.; Wang, H.; Belvitch, P.; Meliton, L.; Bandela, M.; Letsiou, E.; Dudek, S.M. Group V phospholipase A2 mediates endothelial dysfunction and acute lung injury caused by methicillin-resistant Staphylococcus Aureus. *Cells* **2021**, *10*, 1731. [CrossRef] [PubMed]

135. Launay, J.M.; Herve, P.; Callebert, J.; Mallat, Z.; Collet, C.; Doly, S.; Belmer, A.; Diaz, S.L.; Hatia, S.; Cote, F.; et al. Serotonin 5-HT2B receptors are required for bone-marrow contribution to pulmonary arterial hypertension. *Blood* **2012**, *119*, 1772–1780. [CrossRef] [PubMed]
136. Wu, C.; Su, J.; Wang, X.; Wang, J.; Xiao, K.; Li, Y.; Xiao, Q.; Ling, M.; Xiao, Y.; Qin, C.; et al. Overexpression of the phospholipase A2 group V gene in glioma tumors is associated with poor patient prognosis. *Cancer Manag. Res.* **2019**, *11*, 3139–3152. [CrossRef]
137. Li, B.; Yang, H.; Shen, B.; Huang, J.; Qin, Z. Procollagen-lysine, 2-oxoglutarate 5-dioxygenase 1 increases cellular proliferation and colony formation capacity in lung cancer via activation of E2F transcription factor 1. *Oncol. Lett.* **2021**, *22*, 851. [CrossRef]
138. Li, J.; Lam, A.S.M.; Yau, S.T.Y.; Yiu, K.K.L.; Tsoi, K.K.F. Antihypertensive treatments and risks of lung Cancer: A large population-based cohort study in Hong Kong. *BMC Cancer* **2021**, *21*, 1202. [CrossRef]
139. Tian, L.; Zhou, H.; Wang, G.; Wang, W.Y.; Li, Y.; Xue, X. The relationship between PLOD1 expression level and glioma prognosis investigated using public databases. *PeerJ* **2021**, *9*, e11422. [CrossRef]
140. Mehta, M.B.; Shewale, S.V.; Sequeira, R.N.; Millar, J.S.; Hand, N.J.; Rader, D.J. Hepatic protein phosphatase 1 regulatory subunit 3B (Ppp1r3b) promotes hepatic glycogen synthesis and thereby regulates fasting energy homeostasis. *J. Biol. Chem.* **2017**, *292*, 10444–10454. [CrossRef]
141. Oben, A.; Jauk, V.; Battarbee, A.; Longo, S.; Szychowski, J.; Tita, A.; Harper, L. Value of HbA1c in obese women with gestational diabetes. *Am. J. Perinatol.* **2021**. [CrossRef] [PubMed]
142. Panossian, A.; Seo, E.J.; Efferth, T. Novel molecular mechanisms for the adaptogenic effects of herbal extracts on isolated brain cells using systems biology. *Phytomedicine* **2018**, *50*, 257–284. [CrossRef] [PubMed]
143. Tang, Y.; Fung, E.; Xu, A.; Lan, H.Y. C-reactive protein and ageing. *Clin. Exp. Pharmacol. Physiol.* **2017**, *44*, 9–14. [CrossRef] [PubMed]
144. Touraine, P.; Martini, J.F.; Zafrani, B.; Durand, J.C.; Labaille, F.; Malet, C.; Nicolas, A.; Trivin, C.; Postel-Vinay, M.C.; Kuttenn, F.; et al. Increased expression of prolactin receptor gene assessed by quantitative polymerase chain reaction in human breast tumors versus normal breast tissues. *J. Clin. Endocrinol. Metab.* **1998**, *83*, 667–674. [CrossRef]
145. Zhou, W.; Wang, Y.; Gao, H.; Jia, Y.; Xu, Y.; Wan, X.; Zhang, Z.; Yu, H.; Yan, S. Identification of key genes involved in pancreatic ductal adenocarcinoma with diabetes mellitus based on gene expression profiling analysis. *Pathol. Oncol. Res.* **2021**, *27*, 604730. [CrossRef]
146. Zhao, C.Y.; Hua, C.H.; Li, C.H.; Zheng, R.Z.; Li, X.Y. High PYGL expression predicts poor prognosis in human gliomas. *Front. Neurol.* **2021**, *12*, 652931. [CrossRef]
147. Xia, W.; Su, L.; Jiao, J. Cold-induced protein RBM3 orchestrates neurogenesis via modulating Yap mRNA stability in cold stress. *J. Cell Biol.* **2018**, *217*, 3464–3479. [CrossRef]
148. Takahashi, Y.; Hori, M.; Shimoji, K.; Miyajima, M.; Akiyama, O.; Arai, H.; Aoki, S. Changes in delta ADC reflect intracranial pressure changes in craniosynostosis. *Acta Radiol. Open* **2017**, *6*, 2058460117728535. [CrossRef]
149. Jogi, A.; Brennan, D.J.; Ryden, L.; Magnusson, K.; Ferno, M.; Stal, O.; Borgquist, S.; Uhlen, M.; Landberg, G.; Pahlman, S.; et al. Nuclear expression of the RNA-binding protein RBM3 is associated with an improved clinical outcome in breast cancer. *Mod. Pathol.* **2009**, *22*, 1564–1574. [CrossRef]
150. Sarang, Z.; Saghy, T.; Budai, Z.; Ujlaky-Nagy, L.; Bedekovics, J.; Beke, L.; Mehes, G.; Nagy, G.; Ruhl, R.; Moise, A.R.; et al. Retinol saturase knock-out mice are characterized by impaired clearance of apoptotic cells and develop mild autoimmunity. *Biomolecules* **2019**, *9*, 737. [CrossRef]
151. Martin Calderon, L.; Chaudhury, M.; Pope, J.E. Healthcare utilization and economic burden in systemic sclerosis: A systematic review. *Rheumatology* **2021**, keab847. [CrossRef] [PubMed]
152. Zhao, L.; Zhu, X.; Xia, M.; Li, J.; Guo, A.Y.; Zhu, Y.; Yang, X. Quercetin ameliorates gut microbiota dysbiosis that drives hypothalamic damage and hepatic lipogenesis in monosodium glutamate-induced abdominal obesity. *Front. Nutr.* **2021**, *8*, 671353. [CrossRef] [PubMed]
153. Li, R.; Luo, S.Y.; Zuo, Z.G.; Yu, Z.; Chen, W.N.; Ye, Y.X.; Xia, M. Association between serum uric acid to creatinine ratio and metabolic syndrome based on community residents in Chashan town, Dongguan city. *Zhonghua Yu Fang Yi Xue Za Zhi (Chin. J. Prev. Med.)* **2021**, *55*, 1449–1455.
154. Mei, J.; Hu, K.; Peng, X.; Wang, H.; Liu, C. Decreased expression of SLC16A12 mRNA predicts poor prognosis of patients with clear cell renal cell carcinoma. *Medicine* **2019**, *98*, e16624. [CrossRef]
155. Liu, J.; Bao, J.; Zhang, W.; Li, Q.; Hou, J.; Wei, X.; Huang, Y. The potential of visceral adipose tissue in distinguishing clear cell renal cell carcinoma from renal angiomyolipoma with minimal fat. *Cancer Manag. Res.* **2021**, *13*, 8907–8914. [CrossRef]
156. Zuercher, J.; Neidhardt, J.; Magyar, I.; Labs, S.; Moore, A.T.; Tanner, F.C.; Waseem, N.; Schorderet, D.F.; Munier, F.L.; Bhattacharya, S.; et al. Alterations of the 5'untranslated region of SLC16A12 lead to age-related cataract. *Investig. Ophthalmol. Vis. Sci.* **2010**, *51*, 3354–3361. [CrossRef]
157. Ang, M.J.; Afshari, N.A. Cataract and systemic disease: A review. *Clin. Exp. Ophthalmol.* **2021**, *49*, 118–127. [CrossRef]
158. Christensen, H.L.; Barbuskaite, D.; Rojek, A.; Malte, H.; Christensen, I.B.; Fuchtbauer, A.C.; Fuchtbauer, E.M.; Wang, T.; Praetorius, J.; Damkier, H.H. The choroid plexus sodium-bicarbonate cotransporter NBCe2 regulates mouse cerebrospinal fluid pH. *J. Physiol.* **2018**, *596*, 4709–4728. [CrossRef]
159. Betz, M.V.; Nemec, K.B.; Zisman, A.L. Plant-based diets in kidney disease: Nephrology professionals' perspective. *J. Ren. Nutr.* **2021**. [CrossRef]

160. Kant, S.; Stopa, E.G.; Johanson, C.E.; Baird, A.; Silverberg, G.D. Choroid plexus genes for CSF production and brain homeostasis are altered in Alzheimer's disease. *Fluids Barriers CNS* **2018**, *15*, 34. [CrossRef]
161. Coatl-Cuaya, H.; Tendilla-Beltran, H.; de Jesús-Vásquez, L.M.; Garces-Ramirez, L.; Gomez-Villalobos, M.J.; Flores, G. Losartan enhances cognitive and structural neuroplasticity impairments in spontaneously hypertensive rats. *J. Chem. Neuroanat.* **2021**, *120*, 102061. [CrossRef] [PubMed]
162. Yuting, Y.; Lafeng, F.; Qiwei, H. Secreted modular calcium-binding protein 2 promotes high fat diet (HFD)-induced hepatic steatosis through enhancing lipid deposition, fibrosis and inflammation via targeting TGF-β1. *Biochem. Biophys. Res. Commun.* **2019**, *509*, 48–55. [CrossRef] [PubMed]
163. Calvopina, D.A.; Lewindon, P.J.; Ramm, L.E.; Noble, C.; Hartel, G.F.; Leung, D.H.; Ramm, G.A. Gamma-glutamyl transpeptidase-to-platelet ratio as a biomarker of liver disease and hepatic fibrosis severity in paediatric cystic fibrosis. *J. Cyst. Fibros.* **2021**. [CrossRef] [PubMed]
164. Hyun, C.L.; Park, S.J.; Kim, H.S.; Song, H.J.; Kim, H.U.; Lee, C.; Lee, D.H.; Maeng, Y.H.; Kim, Y.S.; Jang, B. The intestinal stem cell marker SMOC2 is an independent prognostic marker associated with better survival in gastric cancer. *Anticancer Res.* **2021**, *41*, 3689–3698. [CrossRef] [PubMed]
165. Gomez-Abenza, E.; Ibanez-Molero, S.; Garcia-Moreno, D.; Fuentes, I.; Zon, L.I.; Mione, M.C.; Cayuela, M.L.; Gabellini, C.; Mulero, V. Zebrafish modeling reveals that SPINT1 regulates the aggressiveness of skin cutaneous melanoma and its crosstalk with tumor immune microenvironment. *J. Exp. Clin. Cancer Res.* **2019**, *38*, 405. [CrossRef]
166. Soffietti, R.; Ruda, R.; Mutani, R. Management of brain metastases. *J. Neurol.* **2002**, *249*, 1357–1369. [CrossRef]
167. Huang, H.P.; Chang, M.H.; Chen, Y.T.; Hsu, H.Y.; Chiang, C.L.; Cheng, T.S.; Wu, Y.M.; Wu, M.Z.; Hsu, Y.C.; Shen, C.C.; et al. Persistent elevation of hepatocyte growth factor activator inhibitors in cholangiopathies affects liver fibrosis and differentiation. *Hepatology* **2012**, *55*, 161–172. [CrossRef]
168. Takashima, Y.; Keino-Masu, K.; Yashiro, H.; Hara, S.; Suzuki, T.; van Kuppevelt, T.H.; Masu, M.; Nagata, M. Heparan sulfate 6-O-endosulfatases, Sulf1 and Sulf2, regulate glomerular integrity by modulating growth factor signaling. *Am. J. Physiol. Renal Physiol.* **2016**, *310*, F395–F408. [CrossRef]
169. Saito, N.; Toyoda, M.; Ono, M.; Kondo, M.; Moriya, H.; Kimura, M.; Sawada, K.; Fukagawa, M. Regulation of blood pressure and phosphorylation of β1-integrin in renal tissue in a rat model of diabetic nephropathy. *Tokai J. Exp. Clin. Med.* **2021**, *46*, 172–179.
170. Lee, H.Y.; Yeh, B.W.; Chan, T.C.; Yang, K.F.; Li, W.M.; Huang, C.N.; Ke, H.L.; Li, C.C.; Yeh, H.C.; Liang, P.I.; et al. Sulfatase-1 overexpression indicates poor prognosis in urothelial carcinoma of the urinary bladder and upper tract. *Oncotarget* **2017**, *8*, 47216–47229. [CrossRef]
171. Chen, J.S.; Lu, C.L.; Huang, L.C.; Shen, C.H.; Chen, S.C. Chronic kidney disease is associated with upper tract urothelial carcinoma: A nationwide population-based cohort study in Taiwan. *Medicine* **2016**, *95*, e3255. [CrossRef] [PubMed]
172. Clarke, W.T.; Edwards, B.; McCullagh, K.J.; Kemp, M.W.; Moorwood, C.; Sherman, D.L.; Burgess, M.; Davies, K.E. Syncoilin modulates peripherin filament networks and is necessary for large-calibre motor neurons. *J. Cell Sci.* **2010**, *123*, 2543–2552. [CrossRef] [PubMed]
173. Silva, P.S.C.D.; Boing, A.F. Factors associated with leisure-time physical activity: Analysis of Brazilians with chronic diseases. *Cien Saude Colet (Sci. Collect. Health)* **2021**, *26*, 5727–5738. [CrossRef] [PubMed]
174. Wang, D.; Deng, L.; Xu, X.; Ji, Y.; Jiao, Z. Elevated SYNC expression is associated with gastric tumorigenesis and infiltration of M2-polarized macrophages in the gastric tumor immune microenvironment. *Genet. Test. Mol. Biomarkers* **2021**, *25*, 236–246. [CrossRef]
175. Hao, X.L.; Gao, L.Y.; Deng, X.J.; Han, F.; Chen, H.Q.; Jiang, X.; Liu, W.B.; Wang, D.D.; Chen, J.P.; Cui, Z.H.; et al. Identification of TC2N as a novel promising suppressor of PI3K-AKT signaling in breast cancer. *Cell Death Dis.* **2019**, *10*, 424. [CrossRef]
176. Xu, J.; Ou, X.; Li, J.; Cai, Q.; Sun, K.; Ye, J.; Peng, J. Overexpression of TC2N is associated with poor prognosis in gastric cancer. *J. Cancer.* **2021**, *12*, 807–817. [CrossRef]
177. Jeng, J.Y.; Harasztosi, C.; Carlton, A.J.; Corns, L.F.; Marchetta, P.; Johnson, S.L.; Goodyear, R.J.; Legan, K.P.; Ruttiger, L.; Richardson, G.P.; et al. MET currents and otoacoustic emissions from mice with a detached tectorial membrane indicate the extracellular matrix regulates Ca2+ near stereocilia. *J. Physiol.* **2021**, *599*, 2015–2036. [CrossRef]
178. Frisina, R.D.; Wheeler, H.E.; Fossa, S.D.; Kerns, S.L.; Fung, C.; Sesso, H.D.; Monahan, P.O.; Feldman, D.R.; Hamilton, R.; Vaughn, D.J.; et al. Comprehensive audiometric analysis of hearing impairment and tinnitus after cisplatin-based chemotherapy in survivors of adult-onset cancer. *J. Clin. Oncol.* **2016**, *34*, 2712–2720. [CrossRef]
179. Solares, C.A.; Edling, A.E.; Johnson, J.M.; Baek, M.J.; Hirose, K.; Hughes, G.B.; Tuohy, V.K. Murine autoimmune hearing loss mediated by CD4+ T cells specific for inner ear peptides. *J. Clin. Investig.* **2004**, *113*, 1210–1217. [CrossRef]
180. Xu, Z.; Ruan, J.; Pan, L.; Chen, C. Candidate genes identified in systemic sclerosis-related pulmonary arterial hypertension were associated with immunity, inflammation, and cytokines. *Cardiovasc. Ther.* **2021**, *2021*, 6651009. [CrossRef]
181. Kiermayer, C.; Northrup, E.; Schrewe, A.; Walch, A.; de Angelis, M.H.; Schoensiegel, F.; Zischka, H.; Prehn, C.; Adamski, J.; Bekeredjian, R.; et al. Heart-specific knockout of the mitochondrial thioredoxin reductase (Txnrd2) induces metabolic and contractile dysfunction in the aging myocardium. *J. Am. Heart Assoc.* **2015**, *4*, e002153. [CrossRef] [PubMed]
182. Liang, J.; Zhu, R.; Yang, Y.; Li, R.; Hong, C.; Luo, C. A predictive model for dilated cardiomyopathy with pulmonary hypertension. *ESC Heart Fail.* **2021**, *8*, 4255–4264. [CrossRef] [PubMed]

183. Mou, D.; Ding, D.; Yan, H.; Qin, B.; Dong, Y.; Li, Z.; Che, L.; Fang, Z.; Xu, S.; Lin, Y.; et al. Maternal supplementation of organic selenium during gestation improves sows and offspring antioxidant capacity and inflammatory status and promotes embryo survival. *Food Funct.* **2020**, *11*, 7748–7761. [CrossRef] [PubMed]
184. Trinchese, G.; Cimmino, F.; Cavaliere, G.; Rosati, L.; Catapano, A.; Sorriento, D.; Murru, E.; Bernardo, L.; Pagani, L.; Bergamo, P.; et al. Heart mitochondrial metabolic flexibility and redox status are improved by donkey and human milk intake. *Antioxidants* **2021**, *10*, 1807. [CrossRef] [PubMed]
185. Busceti, C.L.; Cotugno, M.; Bianchi, F.; Forte, M.; Stanzione, R.; Marchitti, S.; Battaglia, G.; Nicoletti, F.; Fornai, F.; Rubattu, S. Brain overexpression of uncoupling protein-2 (UCP2) delays renal damage and stroke occurrence in stroke-prone spontaneously hypertensive rats. *Int. J. Mol. Sci.* **2020**, *21*, 4289. [CrossRef] [PubMed]
186. Kim, J.W.; Cardin, D.B.; Vaishampayan, U.N.; Kato, S.; Grossman, S.R.; Glazer, P.M.; Shyr, Y.; Ivy, S.P.; LoRusso, P.M. Clinical activity and safety of cediranib and olaparib combination in patients with metastatic pancreatic ductal adenocarcinoma without brca mutation. *Oncologist* **2021**, *26*, e1104–e1109. [CrossRef]
187. Albert, F.W.; Somel, M.; Carneiro, M.; Aximu-Petri, A.; Halbwax, M.; Thalmann, O.; Blanco-Aguiar, J.A.; Plyusnina, I.Z.; Trut, L.; Villafuerte, R.; et al. A comparison of brain gene expression levels in domesticated and wild animals. *PLoS Genet.* **2012**, *8*, e1002962. [CrossRef]
188. Sato, D.X.; Rafati, N.; Ring, H.; Younis, S.; Feng, C.; Blanco-Aguiar, J.A.; Rubin, C.J.; Villafuerte, R.; Hallbook, F.; Carneiro, M.; et al. Brain transcriptomics of wild and domestic rabbits suggests that changes in dopamine signaling and ciliary function contributed to evolution of tameness. *Genome Biol. Evol.* **2020**, *12*, 1918–1928. [CrossRef]
189. Yang, X.; Zhang, H.; Shang, J.; Liu, G.; Xia, T.; Zhao, C.; Sun, G.; Dou, H. Comparative analysis of the blood transcriptomes between wolves and dogs. *Anim. Genet.* **2018**, *49*, 291–302. [CrossRef]
190. Hekman, J.P.; Johnson, J.L.; Edwards, W.; Vladimirova, A.V.; Gulevich, R.G.; Ford, A.L.; Kharlamova, A.V.; Herbeck, Y.; Acland, G.M.; Raetzman, L.T.; et al. Anterior pituitary transcriptome suggests differences in ACTH release in tame and aggressive foxes. *G3* **2018**, *8*, 859–873. [CrossRef]
191. Long, K.; Mao, K.; Che, T.; Zhang, J.; Qiu, W.; Wang, Y.; Tang, Q.; Ma, J.; Li, M.; Li, X. Transcriptome differences in frontal cortex between wild boar and domesticated pig. *Anim. Sci. J.* **2018**, *89*, 848–857. [CrossRef] [PubMed]
192. Yang, Y.; Adeola, A.C.; Xie, H.B.; Zhang, Y.P. Genomic and transcriptomic analyses reveal selection of genes for puberty in Bama Xiang pigs. *Zool. Res.* **2018**, *39*, 424–430. [PubMed]
193. Fallahshahroudi, A.; Lotvedt, P.; Belteky, J.; Altimiras, J.; Jensen, P. Changes in pituitary gene expression may underlie multiple domesticated traits in chickens. *Heredity* **2019**, *122*, 195–204. [CrossRef]
194. Samet, H. A top-down quadtree traversal algorithm. *IEEE Trans. Pattern Anal. Mach. Intell.* **1985**, *7*, 94–98. [CrossRef] [PubMed]
195. Sun, G.-L.; Shen, W.; Wen, J.-F. Triosephosphate Isomerase Genes in Two Trophic Modes of Euglenoids (Euglenophyceae) and Their Phylogenetic Analysis. *J. Eukaryot. Microbiol.* **2008**, *55*, 170–177. [CrossRef] [PubMed]
196. Morozova, O.V.; Alekseeva, A.E.; Sashina, T.A.; Brusnigina, N.F.; Epifanova, N.V.; Kashnikov, A.U.; Zverev, V.V.; Novikova, N.A. Phylodynamics of G4P [8] and G2P [4] strains of rotavirus A isolated in Russia in 2017 based on full-genome analyses. *Virus Genes* **2020**, *56*, 537–545. [CrossRef] [PubMed]
197. Hakizimana, J.N.; Yona, C.; Kamana, O.; Nauwynck, H.; Misinzo, G. African Swine Fever Virus Circulation between Tanzania and Neighboring Countries: A Systematic Review and Meta-Analysis. *Viruses* **2021**, *13*, 306. [CrossRef] [PubMed]
198. Zhang, Y.; Katoh, T.K.; Finet, C.; Izumitani, H.F.; Toda, M.J.; Watabe, H.-A.; Katoh, T. Phylogeny and evolution of mycophagy in the Zygothrica genus group (Diptera: Drosophilidae). *Mol. Phylogenetics Evol.* **2021**, *163*, 107257. [CrossRef]
199. Crowley, J.P.; Metzger, J.B.; Merrill, E.W.; Valeri, C.R. Whole blood viscosity in beta thalassemia minor. *Ann. Clin. Lab. Sci.* **1992**, *22*, 229–235.
200. Philibert, C.; Bouillot, S.; Huber, P.; Faury, G. Protocadherin-12 deficiency leads to modifications in the structure and function of arteries in mice. *Pathol. Biol.* **2012**, *60*, 34–40. [CrossRef]
201. Mukai, S.; Oue, N.; Oshima, T.; Imai, T.; Sekino, Y.; Honma, R.; Sakamoto, N.; Sentani, K.; Kuniyasu, H.; Egi, H.; et al. Overexpression of PCDHB9 promotes peritoneal metastasis and correlates with poor prognosis in patients with gastric cancer. *J. Pathol.* **2017**, *243*, 100–110. [CrossRef] [PubMed]
202. Ponomarenko, M.; Rasskazov, D.; Chadaeva, I.; Sharypova, E.; Drachkova, I.; Oshchepkov, D.; Ponomarenko, P.; Savinkova, L.; Oshchepkova, E.; Nazarenko, M.; et al. Candidate SNP markers of atherogenesis significantly shifting the affinity of TATA-binding protein for human gene promoters show stabilizing natural selection as a sum of neutral drift accelerating atherogenesis and directional natural selection slowing it. *Int. J. Mol. Sci.* **2020**, *21*, 1045. [CrossRef] [PubMed]
203. Ponomarenko, M.; Rasskazov, D.; Arkova, O.; Ponomarenko, P.; Suslov, V.; Savinkova, L.; Kolchanov, N. How to use SNP_TATA_Comparator to find a significant change in gene expression caused by the regulatory SNP of this gene's promoter via a change in affinity of the TATA-binding protein for this promoter. *Biomed. Res. Int.* **2015**, *2015*, 359835. [CrossRef] [PubMed]
204. Varzari, A.; Tudor, E.; Bodrug, N.; Corloteanu, A.; Axentii, E.; Deyneko, I.V. Age-specific association of CCL5 gene polymorphism with pulmonary tuberculosis: A case-control study. *Genet. Test. Mol. Biomark.* **2018**, *22*, 281–287. [CrossRef] [PubMed]
205. Cho, S.N.; Choi, J.A.; Lee, J.; Son, S.H.; Lee, S.A.; Nguyen, T.D.; Choi, S.Y.; Song, C.H. Ang II-Induced hypertension exacerbates the pathogenesis of tuberculosis. *Cells* **2021**, *10*, 2478. [CrossRef] [PubMed]
206. Haeussler, M.; Raney, B.; Hinrichs, A.; Clawson, H.; Zweig, A.; Karolchik, D.; Casper, J.; Speir, M.; Haussler, D.; Kent, W. Navigating protected genomics data with UCSC Genome Browser in a box. *Bioinformatics* **2015**, *31*, 764–766. [CrossRef] [PubMed]

207. Stajich, J.E.; Block, D.; Boulez, K.; Brenner, S.E.; Chervitz, S.A.; Dagdigian, C.; Fuellen, G.; Gilbert, J.G.; Korf, I.; Lapp, H.; et al. The Bioperl toolkit: Perl modules for the life sciences. *Genome Res.* **2002**, *12*, 1611–1618. [CrossRef]
208. Waardenberg, A.; Basset, S.; Bouveret, R.; Harvey, R. CompGO: An R package, for comparing and visualizing Gene Ontology enrichment differences between DNA binding experiments. *BMC Bioinform.* **2015**, *16*, 275. [CrossRef]
209. Zerbino, D.; Wilder, S.; Johnson, N.; Juettemann, T.; Flicek, P. The Ensembl regulatory build. *Genome Biol.* **2015**, *16*, 56. [CrossRef]
210. Day, I.N. dbSNP in the detail and copy number complexities. *Hum. Mutat.* **2010**, *31*, 2–4. [CrossRef]
211. Martiney, J.A.; Cerami, A.; Slater, A.F. Inhibition of hemozoin formation in Plasmodium falciparum trophozoite extracts by heme analogs: Possible implication in the resistance to malaria conferred by the beta-thalassemia trait. *Mol. Med.* **1996**, *2*, 236–246. [CrossRef] [PubMed]
212. Ponomarenko, P.; Savinkova, L.; Drachkova, I.; Lysova, M.; Arshinova, T.; Ponomarenko, M.; Kolchanov, N. A step-by-step model of TBP/TATA box binding allows predicting human hereditary diseases by single nucleotide polymorphism. *Dokl. Biochem. Biophys.* **2008**, *419*, 88–92. [CrossRef] [PubMed]
213. Delgadillo, R.; Whittington, J.; Parkhurst, L.; Parkhurst, L. The TBP core domain in solution variably bends TATA sequences via a three-step binding mechanism. *Biochemistry* **2009**, *48*, 1801–1809. [CrossRef] [PubMed]
214. Hahn, S.; Buratowski, S.; Sharp, P.; Guarente, L. Yeast TATA-binding protein TFIID binds to TATA elements with both consensus and nonconsensus DNA sequences. *Proc. Natl. Acad. Sci. USA* **1989**, *86*, 5718–5722. [CrossRef]
215. Karas, H.; Knuppel, R.; Schulz, W.; Sklenar, H.; Wingender, E. Combining structural analysis of DNA with search routines for the detection of transcription regulatory elements. *Comput. Applic. Biosci.* **1996**, *12*, 441–446. [CrossRef]
216. Ponomarenko, M.P.; Ponomarenko, J.V.; Frolov, A.S.; Podkolodny, N.L.; Savinkova, L.K.; Kolchanov, N.A.; Overton, G.C. Identification of sequence-dependent features correlating to activity of DNA sites interacting with proteins. *Bioinformatics* **1999**, *15*, 687–703. [CrossRef]
217. Bucher, P. Weight matrix descriptions of four eukaryotic RNA polymerase II promoter elements derived from 502 unrelated promoter sequences. *J. Mol. Biol.* **1990**, *212*, 563–578. [CrossRef]
218. Flatters, D.; Lavery, R. Sequence-dependent dynamics of TATA-Box binding sites. *Biophys. J.* **1998**, *75*, 372–381. [CrossRef]
219. Ponomarenko, P.M.; Suslov, V.V.; Savinkova, L.K.; Ponomarenko, M.P.; Kolchanov, N.A. A precise equilibrium equation for four steps of binding between TBP and TATA-box allows for the prediction of phenotypical expression upon mutation. *Biophysics* **2010**, *55*, 358–369. [CrossRef]
220. Mogno, I.; Vallania, F.; Mitra, R.D.; and Cohen, B.A. TATA is a modular component of synthetic promoters. *Genome Res.* **2010**, *20*, 1391–1397. [CrossRef]
221. Pugh, B. Purification of the human TATA-binding protein, TBP. *Methods Mol. Biol.* **1995**, *37*, 359–367.
222. Savinkova, L.; Drachkova, I.; Arshinova, T.; Ponomarenko, P.; Ponomarenko, M.; Kolchanov, N. An experimental verification of the predicted effects of promoter TATA-box polymorphisms associated with human diseases on interactions between the TATA boxes and TATA-binding protein. *PLoS ONE* **2013**, *8*, e54626.
223. Drachkova, I.; Savinkova, L.; Arshinova, T.; Ponomarenko, M.; Peltek, S.; Kolchanov, N. The mechanism by which TATA-box polymorphisms associated with human hereditary diseases influence interactions with the TATA-binding protein. *Hum. Mutat.* **2014**, *35*, 601–608. [CrossRef] [PubMed]
224. Kimura, M. A simple method for estimating evolutionary rates of base substitutions through comparative studies of nucleotide sequences. *J. Mol. Evol.* **1980**, *16*, 111–120. [CrossRef]
225. Li, W.H.; Wu, C.I.; Luo, C.C. A new method for estimating synonymous and nonsynonymous rates of nucleotide substitution considering the relative likelihood of nucleotide and codon changes. *Mol. Biol. Evol.* **1985**, *2*, 150–174. [PubMed]
226. Oggenfuss, U.; Badet, T.; Wicker, T.; Hartmann, F.E.; Singh, N.K.; Abraham, L.; Karisto, P.; Vonlanthen, T.; Mundt, C.; McDonald, B.A.; et al. A population-level invasion by transposable elements triggers genome expansion in a fungal pathogen. *eLife* **2021**, *10*, e69249. [CrossRef] [PubMed]
227. Kasowski, M.; Grubert, F.; Heffelfinger, C.; Hariharan, M.; Asabere, A.; Waszak, S.; Habegger, L.; Rozowsky, J.; Shi, M.; Urban, A.; et al. Variation in transcription factor binding among humans. *Science* **2010**, *328*, 232–235. [CrossRef]
228. 1000 Genomes Project Consortium; Abecasis, G.; Auton, A.; Brooks, L.; DePristo, M.; Durbin, R.; Handsaker, R.; Kang, H.; Marth, G.; McVean, G.; et al. An integrated map of genetic variation from 1.092 human genomes. *Nature* **2012**, *491*, 56–65.
229. Haldane, J.B.S. The cost of natural selection. *J. Genet.* **1957**, *55*, 511–524. [CrossRef]
230. Kimura, M. Evolutionary rate at the molecular level. *Nature* **1968**, *217*, 624–626. [CrossRef]
231. Hill, A.E.; Plyler, Z.E.; Tiwari, H.; Patki, A.; Tully, J.P.; McAtee, C.W.; Moseley, L.A.; Sorscher, E.J. Longevity and plasticity of CFTR provide an argument for noncanonical SNP organization in hominid DNA. *PLoS ONE* **2014**, *9*, e109186. [CrossRef] [PubMed]
232. Naumenko, E.; Popova, N.; Nikulina, E.; Dygalo, N.; Shishkina, G.; Borodin, P.; Markel, A. Behavior, adrenocortical activity, and brain monoamines in Norway rats selected for reduced aggressiveness towards man. *Pharmacol. Biochem. Behav.* **1989**, *33*, 85–91. [CrossRef]
233. Paxinos, G.; Watson, C.R. *The Rat Brain in Stereotaxic Coordinates*, 7th ed.; Academic Press: London, UK, 2013; p. 472.
234. Bolger, A.M.; Lohse, M.; Usadel, B. Trimmomatic: A flexible trimmer for Illumina sequence data. *Bioinformatics* **2014**, *30*, 2114–2120. [CrossRef] [PubMed]
235. Kim, D.; Pertea, G.; Trapnell, C.; Pimentel, H.; Kelley, R.; Salzberg, S.L. TopHat2: Accurate alignment of transcriptomes in the presence of insertions, deletions and gene fusions. *Genome Biol.* **2013**, *14*, 36. [CrossRef]

236. Li, H.; Handsaker, B.; Wysoker, A.; Fennell, T.; Ruan, J.; Homer, N.; Marth, G.; Abecasis, G.; Durbin, R. The Sequence alignment/map (SAM) format and SAMtools. *Bioinformatics* **2009**, *25*, 2078–2079. [CrossRef]
237. Anders, S.; Pyl, P.T.; Huber, W. HTSeq—A Python framework to work with high-throughput sequencing data. *Bioinformatics* **2015**, *31*, 166–169. [CrossRef]
238. Love, M.I.; Huber, W.; Anders, S. Moderated estimation of fold change and dispersion for RNA-seq data with DESeq2. *Genome Biol.* **2014**, *15*, 550. [CrossRef]
239. Anders, S.; Huber, W. Differential expression analysis for sequence count data. *Genome Biol.* **2010**, *11*, 106. [CrossRef]
240. Ye, J.; Coulouris, G.; Zaretskaya, I.; Cutcutache, I.; Rozen, S.; Madden, T.L. Primer-BLAST: A tool to design target-specific primers for polymerase chain reaction. *BMC Bioinform.* **2012**, *13*, 134. [CrossRef]
241. Tian, L.; Chen, Y.; Wang, D.W.; Liu, X.H. Validation of reference genes via qRT-PCR in multiple conditions in brandt's voles, lasiopodomys brandtii. *Animals* **2021**, *11*, 897. [CrossRef]
242. Zamani, A.; Powell, K.L.; May, A.; Semple, B.D. Validation of reference genes for gene expression analysis following experimental traumatic brain injury in a pediatric mouse model. *Brain Res. Bull.* **2020**, *156*, 43–49. [CrossRef] [PubMed]
243. Gholami, K.; Loh, S.Y.; Salleh, N.; Lam, S.K.; Hoe, S.Z. Selection of suitable endogenous reference genes for qPCR in kidney and hypothalamus of rats under testosterone influence. *PLoS ONE* **2017**, *12*, e0176368. [CrossRef] [PubMed]
244. Penning, L.C.; Vrieling, H.E.; Brinkhof, B.; Riemers, F.M.; Rothuizen, J.; Rutteman, G.R.; Hazewinkel, H.A. A validation of 10 feline reference genes for gene expression measurements in snap-frozen tissues. *Vet. Immunol. Immunopathol.* **2007**, *120*, 212–222. [CrossRef] [PubMed]